ktu
1922

KAUNAS UNIVERSITY OF TECHNOLOGY

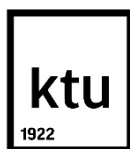**FACULTY OF CHEMICAL TECHNOLOGY**

Artiom Magomedov

SYNTHESIS OF HYDRAZONE AND CARBAZOLYL-BASED CHARGE TRANSPORTING MATERIALS UTILIZING CLICK CHEMISTRY METHODS

Master's thesis

Supervisor

Prof. dr. Vytautas Getautis

Kaunas, 2015

ktu
1922

KAUNO TECHNOLOGIJOS UNIVERSITETAS
CHEMINĖS TECHNOLOGIJOS FAKULTETAS

Artiom Magomedov

KLIK CHEMIJOS METODŲ NAUDOJIMAS HIDRAZONO BEI KARBAZOLILFRAGMENTUS TURINČIŲ KRŪVININKUS TRANSPORTUOJANČIŲ JUNGINIŲ SINTEZĖJE

Baigiamasis magistro darbas

Vadovas

Prof. dr. Vytautas Getautis

Kaunas, 2015

KAUNO TECHNOLOGIJOS UNIVERSITETAS

CHEMINĖS TECHNOLOGIJOS FAKULTETAS

ORGANINĖS CHEMIJOS KATEDRA

TVIRTINU

Organinės chemijos
katedros vedėjas
Prof. dr. Vytas Martynaitis

KLIK CHEMIJOS METODŲ NAUDOJIMAS HIDRAZONO BEI KARBAZOLILFRAGMENTUS TURINČIŲ KRŪVININKUS TRANSPORTUOJANČIŲ JUNGINIŲ SINTEZĖJE

Baigiamasis magistro darbas

Studijų programa Taikomoji chemija (kodas 612F10003)

Darbą atliko
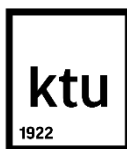
Artiom Magomedov

Vadovas

Prof. dr. Vytautas Getautis

Recenzentas

Prof. dr. Saulius Grigalevičius

Kaunas, 2015

KAUNO TECHNOLOGIJOS UNIVERSITETAS

CHEMINĖS TECHNOLOGIJOS FAKULTETAS

Artiom Magomedov

Studijų programa Taikomoji chemija (kodas 612F10003)

Baigiamojo darbo „ Klik chemijos metodų naudojimas hidrazono bei karbazolilfragmentus turinčių krūvininkus transportuojančių junginių sintezėje “

AKADEMINIO SĄŽININGUMO DEKLARACIJA

2015 m. gegužės mėn. 30 d.

Kaunas

Patvirtinu, kad mano **Artiom Magomedov** baigiamasis darbas tema „*Klik chemijos metodų naudojimas hidrazono bei karbazolilfragmentus turinčių krūvininkus transportuojančių junginių sintezėje*“ yra parašytas visiškai savarankiškai, o visi pateikti duomenys ar tyrimų rezultatai yra teisingi ir gauti sąžiningai. Šiame darbe nei viena darbo dalis nėra plagijuota nuo jokių spausdintinių ar internetinių šaltinių, visos kitų šaltinių tiesioginės ir netiesioginės citatos nurodytos literatūros nuorodose. Įstatymu nenumatytų piniginių sumų už šį darbą niekam nesu mokėjęs.

Aš suprantu, kad išaiškėjus nesąžiningumo faktui, man bus taikomos nuobaudos, remiantis Kauno technologijos universitete galiojančia tvarka.

_____   _____
(studento vardas ir pavardė, įrašyti ranka)   (parašas)

CONTENTS

Magomedov, A. Klik chemijos metodų naudojimas hidrazono bei karbazolilfragmentus turinčių krūvininkus transportuojančių junginių sintezėje. Magistro baigiamasis darbas / vadovas prof. dr. Vytautas Getautis; Kauno technologijos universitetas, Cheminės technologijos fakultetas, Organinės chemijos katedra.

Kaunas, 2015. 65 psl.

SANTRAUKA

Kiekvieną dieną su Saulės šviesa Žemės paviršių pasiekia milžiniški energijos kiekiai. Per metus jie dvigubai viršija visą iš iškastinio kuro (akmens anglies, naftos, gamtinių dujų ir urano) galima išgauti energiją. Išsenkant neatsinaujinantiems energijos šaltiniams vis patraukliau atrodo tiesioginis elektros išgavimas iš Saulės šviesos.

Platesnį saulės elementų paplitimą stabdo aukšta įrenginių kaina ir lėtas atsiperkamumas. Vienintelė skatinanti priemonė investuoti į saulės energetiką yra valstybės subsidijos. Aukštą saulės elementų kainą lemia sudėtinga ir brangių įrenginių reikalaujanti silicio gryninimo technologija. Mažėjantis iškastinio kuro kiekis ir atsinaujinančių energijos šaltinių svarba skatina ieškoti pigesnių ir efektyvesnių technologijų bei medžiagų. Potencialiai pigesnius sprendimus gali pasiūlyti organiniai ir hibridiniai saulės elementai.

2012 metais Henris Snaitas ir Michaelis Graetzelis paskelbė apie naujo tipo saulės elementus, kurių efektyvumas siekė 9-11%. Kaip šviesą sugerenti medžiaga buvo panaudotas metilamonio švino (II) jodido perovskitas. Per 2 metus perovskitiniai saulės elementai viršijo 20% efektyvumo ribą, ir pagal šį rodiklį tapo konkurencingi silicio elementams. Greitą įvedimą į rinką stabdo keletas problemų. Viena iš jų - aukšta skyles transportuojančios medžiagos kaina.
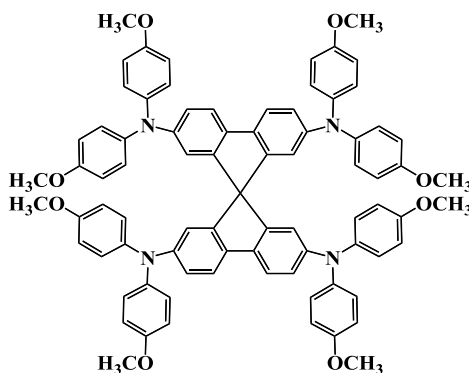
Geriausiu veikimu pasižymi saules elementai su 2,2',7,7'-tetra-(*N*,*N*-di-*p*-metoksifenilamino)-9,9'-spirobifluorenu. Šios medžiagos sintezė yra daugiapakopė, naudojami jautrus ir nuodingi reagentai.

Ankstesniuose tyrymuose buvo išbandyta "Klik" reakcija organinių puslaidininkių sintezei. Hidrazonui su nepakeistu vandeniliu prie azoto atomo reaguojant su bromometilbenzeno dariniais buvo gauti šakotos struktūros junginiai. Šiame darbe buvo tęsiami tyrimai šioje srityje. Susintetinta 13 šakotų hidrazonų bei nustatytos priklausomybės tarp struktūros ir makroskopinių savybių. Taipogi panaudojant bifunkcinius junginius ši strategija buvo pritaikyta polimerų sintezei. Perovskitiniai saulės elementai su šiomis medžiagomis nerodė efektyvumo.

16,91%
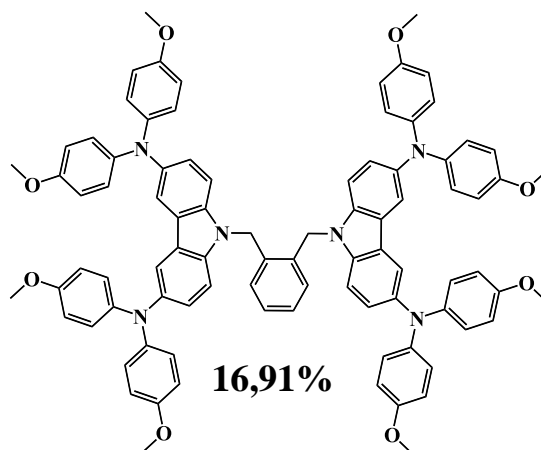
Tęsiant tyrimus ir siekiant gauti efektyvias medžiagas buvo atlikta keletas pakeitimų sintezės schemoje. Vietoje hidrazono buvo naudojamas 3,6-dibromokarbazolas. Halogeno atomai ledo antroje stadijoje įvesti difenilamino fragmentą.

Su 1,2-bis[3,6-(4,4-dimetoksidifenilamino)-9*H*-karbazol-9-metil]benzenu pasiektas vienas geriausių saulės šviesos konversijos efektyvumų (16,91%) perovskitiniuose saulės elementuose su mažamolekulinėmis skyles transportuojančiomis medžiagomis.

LIST OF ABBREVIATIONS AND PHYSICAL UNITS

δ	chemical shift in parts per million;
μ_0	zero field charge carrier mobility;
μ	charge carrier mobility;
^{1}H NMR	proton nuclear magnetic resonance;
^{13}C NMR	carbon nuclear magnetic resonance;
AgTFSI	bis(trifluoromethane)sulfonamide silver salt;
Ar	aromatic and heteroaromatic;
BHJ	bulk heterojunction;
CT	charge transfer;
DCM	dichloromethane;
DMSO	dimethylsulfoxide;
DSC	differential scanning calorimetry;
DSSC	dye sensitized solar cell;
E	electric field;
EDOT	3,4-ethylenedioxythiophene;
FK102	tris(2-(1*H*-pyrazol-1-yl)pyridine)cobalt(III);
GPC	gel permeation chromatography;
HOMO	highest occupied molecular orbital;
HTM	hole transporting material;
I_p	ionization potential;
IR	infrared;
IV-CT	intervalence charge transfer band;
J	coupling constant in Hz;
LiTFSI	bis(trifluoromethane)sulfonimide lithium salt;
LUMO	lowest unoccupied molecular orbital;
m.p.	melting point;

Mn	Number average molecular weight;
NIR	near-infrared;
NMR	nuclear magnetic resonance;
P3HT	poly(3-hexylthiophene-2,5-diyl);
PTAA	poly(triaryl amine);
SC	solar cell;
Spiro-OMeTAD	2,2',7,7'-tetrakis-(N,N-di-p-methoxyphenylamine)-9,9'-spirobifluorene;
ssDSSC	solid-state dye-sensitized solar cell;
t	time;
T	temperature;
T_d	destruction temperature;
T_g	glass transition temperatures;
T_m	melting point;
tBP	4-$tert$-butylpyridine;
TCO	transparent conducting oxide;
TFSI	bis(trifluoromethane)sulfonamide;
THF	tetrahydrofurane;
TLC	thin layer chromatography;
TMS	trimethylsilane;
TPA	triphenylamine;
UV/Vis/NIR	ultraviolet/visible/near-infrared;
XTOF	xerographic time of flight technique.

1. INTRODUCTION

Every day with the sunlight huge amount of energy reaches surface of the Earth. Just imagine, in a year it is twice as large as total reserves of non-renewable energy sources (such as coal, oil, natural gas and uranium) [1]. As fossil fuel goes to the end it looks very attractive to produce electricity directly from the sunlight.

More and more solar plants appear all around the world, but there is an important stopping factor. Although silicone solar cells have in general moderate to good performance (~20-25% energy conversion efficiency) they are still too expensive due to the difficult technology of silicon purification. High price and long payback period makes this business strongly dependent on the government subsidies. So the search of the new materials is crucial for the technological progress.

Recently perovskite solar cells made a splash in a scientific community. They can be prepared by a solution processes, manufacturing can be easily scaled up, and what is the most important in a several years efficiencies reached 20%. But every light has its shadow. One of the drawbacks – high price of the hole transporting material (HTM).

This work concentrates on the search of the alternative to the best HTM - 2,2',7,7'-tetrakis-(*N*,*N*-di-*p*-methoxyphenylamine)-9,9'-spirobifluorene. The final product should be easily prepared and isolated. That is why "Click" chemistry philosophy was adopted for the fast and versatile synthesis.

 Aim of this work: to synthesize novel inexpensive and efficient hole transporting materials for the perovskite solar cells.

Tasks:
1. To synthesize and investigate branched hydrazones by "click" chemistry reaction.
2. To synthesize and investigate hydrazone-based polymers.
3. To synthesize and investigate diphenylamine substituted carbazole twin molecules.

2. LITERATURE REVIEW

2.1.   Organic materials in solar cells

The early investigations of the organic materials for the applications in solar cells were inspired by natural photosynthesis process. It starts with the chlorophyll molecule absorption of the photon and is followed by the charge separation. Plants are using energy of the sun to synthesize carbon-carbon bonds. For us it is more relevant to directly use movement of electrons to produce electricity.
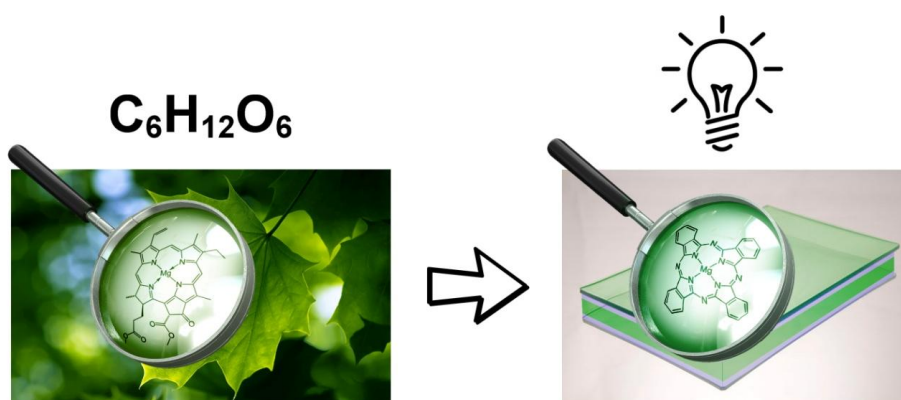

Figure 1 First organic solar cell inspired by nature

First attempts to use organic materials for the sun energy conversion into electricity were made in the 1958 [2]. The cell was made of magnesium phthalocyanine disc coated with a thin film of air oxidized tetramethyl *p*-phenylenediamine (**Figure 1**). Maximum voltage was 200 mV, but efficiency of this cell was very low. Main limitation was the high internal cell resistance. Nevertheless, for the first time it was shown that photovoltaic effect can be observed in pure organic systems. In 1974 some improvement was achieved by changing contacts to metals. Still, efficiency was only about 0.01% [3].

Direct using materials from the plants were also tested in 1975 by C.W. Tang and A.C. Albrecht [4]. Single layer of a microcrystalline chlorophyll-a, coated with metal electrodes were constructed in a similar manner as in previous investigations. As it can be expected, due to the same reasons efficiency again was very low.
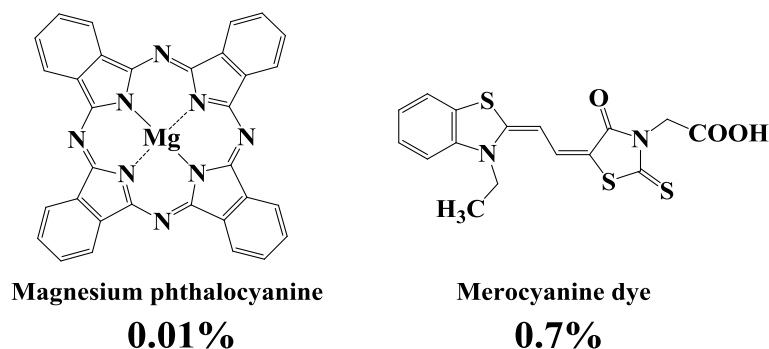
Magnesium phthalocyanine

0.01%

Merocyanine dye

0.7%

Figure 2. Materials used in the single layer organic solar cells

One of the best results for single layer organic solar cells was obtained in 1978. As light absorbing layer merocyanine dye (**Figure 2**) were used and the interfacial oxide layer between metal and dye was added. For the best cell power conversion efficiency reached 0.7% [5].

Although the first results were promising and some improvements were achieved, such devices suffered from the high exciton recombination due to the low electric field generated by electrodes. It is simply not enough to overcome exciton binding energy. Thus vast majority of energy are not converted into electricity and wasted.

The first significant improvement was made with introduction of the heterojunction concept. In this case two layers of electron donor and electron acceptor are used. Differences in electron affinities at surface promote dissociation of the exciton. In 1986 1% efficiency [6] was achieved. Limitation for the further progress was exciton diffusion length. Typically for organic materials it lays in a range of 10 nm. But in order to absorb enough light the layer should be at least 100 nm. It means that only excitons generated near the interface will dissociate. Others will recombine reducing overall performance of the device.

To overcome this limitation it was proposed to make interfaces at the nano-scale. In a scientific literature it has name "bulk heterojunction" (or BHJ) [7]. Ideally it can be made by forming nanostructures (wires, or walls), with at least one dimension near to 10-20 nm. That would provide very large surface area and support that fact that all excitons are generated near the interface (**Figure 3**). In the real heterojunctions a lot of imperfections occur (c.a. inhomogenity of the layers, differences in sizes etc.). With the development of lithography and by optimizing solution processes better results can be obtained.
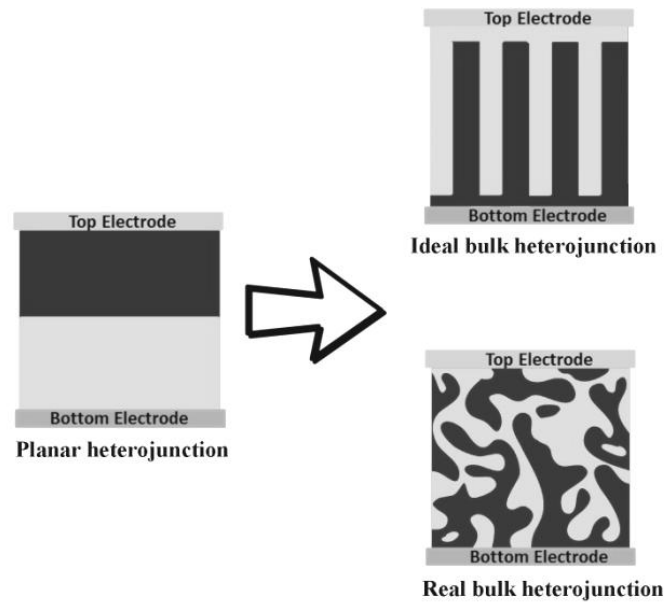
Figure 3. Bulk heterojunction concept

Another way of reducing recombination were proposed in 1991 by Grätzel and O'Regan Dye sensitized solar cells (DSSC, also known as the Grätzel cell) employs an organic dye monolayer, absorbed on a mesoporous TiO_2 scaffold. Large surface area provides good absorption of light. TiO_2 also provides fast electron transport from dye to an electrode. Resulting oxidized dye is then regenerated by the liquid electrolyte (I_2/I_3^-). Already in the first publication incredible 7.9% efficiency was reported [8]. After several years it reached ~11% efficiencies, but then saturation came [9].

Important change in construction of DSSC was made in 1998 by replacing liquid electrolyte with the solid hole transporting material (HTM) [10]. Resulting solid state dye sensitized solar cells (ssDSSC) shows lower efficiencies (usually around 3-5% [11], up to 8% [12]) but are more promising from the practical point of view, as they prevents leakage of the highly corrosive iodine electrolyte.

Recently solar cells again attracted lots of attention from the scientists all over the world. Perovskite solar cells made revolution and in three years overcome 20% efficiency (**Figure 4**), what makes them competitive with silicone solar cells [13].
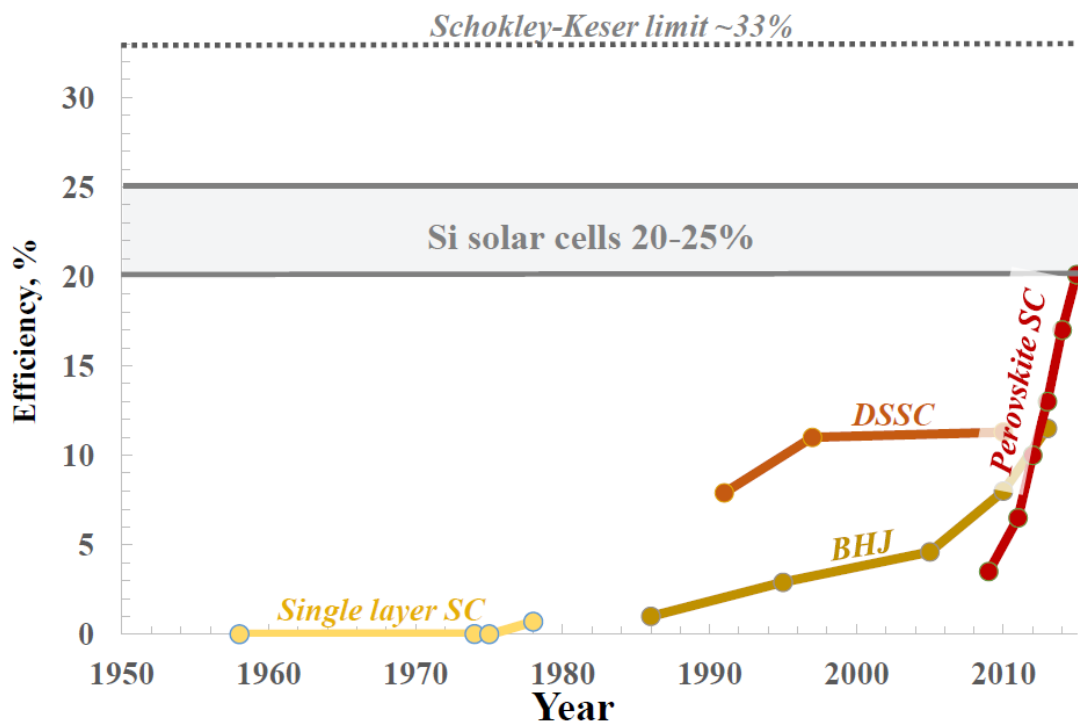
Figure 4. Technological progress and benchmarks of the organic and hybrid solar cells [9]

2.2.   Perovskite Solar Cells – (r)evolution

Original perovskite is a CaTiO$_3$ mineral named after Russian mineralogist Lev Perovski (rus.: *Лев Алексеевич Перовский*). Nowadays this name is used for all materials with the same crystalline structure as in CaTiO$_3$ [14]. In a context of solar energetics perovskite states for the hybrid organic inorganic material (large metal cation, small organic cation and halide anions). If not specially mentioned, in this work perovskite would mean lead halide methylamine perovskite [15].

Perovskite solar cells originally evolved from the DSSC technology. Organic dyes usually have intensive, but narrow absorption bands. In order to increase absorbance of the light in the wider spectral range scientists started to sensitize TiO$_2$ with thin layer of inorganic absorber (quantum dots). First attempts to replace dye with perovskite were made in 2006-2008 years by T. Miyasaka [16], but did not achieve much attention. First report in peer-reviewed journal was in 2009 [17]. At that time 3.8% efficiency was achieved. After two years 6.5% efficiencies were reported [18]. However cells with liquid electrolyte were extremely unstable due to solubility of the perovskite in organic solvent.

Real breakthrough was made in 2012 by Snaith and Gratzel [19, 20]. They replaced liquid electrolyte with 2,2',7,7'-tetrakis-(*N*,*N*-di-*p*-methoxyphenylamine)-9,9'-spirobifluorene (**Spiro-OMeTAD**) solid electrolyte in the same manner as in ssDSSC and achieved 9-11% efficiencies.

This did not left unnoticed and today dozens of scientific groups are working in attempt to increase performance of the perovskite solar cells (**Figure 5**). Up to day 20% limit is already reached. Some technical points will be reviewed in brief.
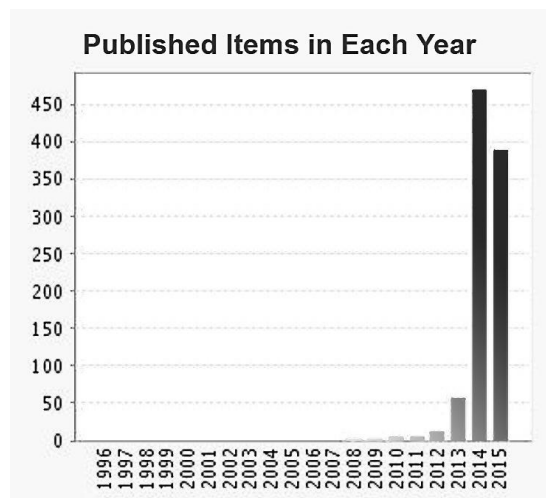

Published Items in Each Year

Figure 5. Publications on the topic "Perovskite solar cells". Data from Thomson Reuters Web of Knowledge citation report (2015-05-28)

2.2.1. Architectures

Interesting point is a development of the perovskite solar cells architecture. Originating from the DSSC and ssDSSC, when only absorber layer were changed, it is now making its own way. TiO_2 mesoporous layer became optional. Solar cells with mesoporous non-conductive Al_2O_3 layer instead of TiO_2 still show good performance. In this case electron conduction is performed by perovskite layer itself. Further simplifications were also made to the flat heterojunction architecture (**Figure 6**). It was even shown that perovskite solar cells can operate without HTM layer [21]. Fortunately to us such devices show lower performance (only up to 10%).
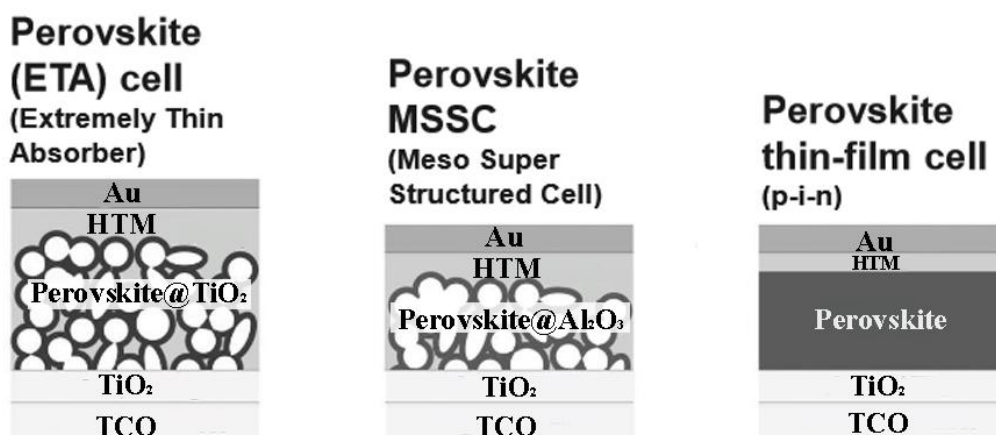

Figure 6. Perovskite solar cell architecture development [22]

2.2.2. Deposition techniques

What also makes perovskite solar cells such attractive is a large variety of layer formation techniques. One way to prepare metylamonium lead-halyde perovskite is a solution processes. The most common technique is a spin coating in different variations. Most simple is to spincoat mixture of lead halide and methilamonium halide and anneal it at 1000^oC [23]. Two compounds can also be covered one on top another and after diffusion perovskite layer is formed. Finally, methylamonium iodine can be inserted into PbI_2 by dipping [24] or from vapor [25]. Other way – vapor deposition of all components [26]. Again it can be done in a various combinations, with mixed halogen ions, at the different deposition times etc. [27].

2.2.3. Issues

Perovskite solar cells are showing very promising performance. But on the way to the commercial products there are still some issues that have to be overcome.

- Reproducibility. At this point the reproducibility is not very good. The efficiencies for the series of the cells prepared under the same conditions can differ in a range up to 5% [28]. Better understanding of the processes is needed.
- Stability. Perovskite itself is very sensitive to the moisture and oxygen. Also such materials as bis(trifluoromethane)sulfonimide lithium salt (**LiTFSI**) even further increase moisture sensitivity. Careful encapsulation can overcome this issue [29].
- Ecology. Possible lead leakage increase importance of the right utilization of the waste. Possible solution – changing lead by a less harmful tin [30].
- High price. The price of the most popular organic HTM **Spiro-OMeTAD** is very high. It can double price of the device [31]. Alternative cheaper materials are of the high importance.

2.3. Spiro-OMeTAD as a HTM in perovskite solar cells

The group of J. Salbeck in 1997 published an article with an application of 9,9'-spirobifluorene based compounds as blue emitters for OLED [32] (**Figure 7**). One year later Grätzel *et al.* published in Nature on the first effective solid-state dye-sensitized mesoporous TiO_2 solar cells with **Spiro-OMeTAD** as an HTM (efficiency 0.74%) [33]. In details photophysical properties of this compound were investigated by Udo Bach in his PhD thesis [34].
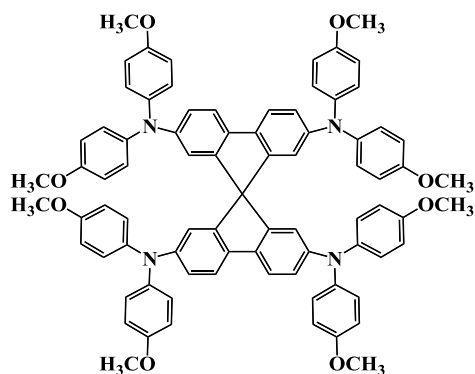
Figure 7. **Spiro-OMeTAD** – most popular HTM for ssDSSC and perovskite solar cells

Up to date it is the most studied hole transporting material for the application in both ssDSSC and perovskite solar cells. All record efficiencies were achieved by using **Spiro-OMeTAD**. While testing new potential HTM's usual strategy is to compare efficiency with the device prepared under the same conditions using **Spiro-OMeTAD**. That is why we will review in more details synthesis and properties of this compound.

2.3.1. Synthesis

Synthesis of the spiro-based compounds can be relatively divided into two stages: synthesis of the 9,9'-spirobifluorene and further fictionalization with diphenylamine moiety [35].

For the first time the unsubstituted 9,9'-spirobifluorene was synthesized in 1930 by R. G. Clarkson and M. Gomberg [36]. 9,'9-spirobifluorene synthesis usually starts from the 2-halogen-biphenyle. After metallization (Mg or Li [37]) 9-fluorenone is added and the intermediate 9-(biphenyl-2-yl)-9-fluorenol is generated. Consequentially catalytic amount of hydrochloric acid is added what leads to a ring-closure reaction. Overall yield for this stage differ from 19% to 90% [35-38].

At the next stage 9,9'-spirobifluorene is halogenated to introduce reactive groups (usually Br [39]) and consequentially Pd-catalized reactions can be used to obtain final product (*e.g.* Buchwald-Hartwig reaction for the functionalization with diarylamine [40]).

As a rule, higher yields require more sensitive and more expensive compounds. In contrary, if one uses readily available starting materials, yield is lower. It makes very difficult to reduce price of the final product.

One of the possible synthesis routes is shown in **Figure 8**.

Figure 8. One of the possible **Spiro-OMeTAD** synthesis scheme

2.3.2. Additives

In a device HTM should provide fast charge transfer from the absorbing layer to the electrode. As most of the organic HTM's **Spiro-OMeTAD** have very low conductivity ($\sim 10^{-8}$ Sm/cm [41]). It results in a high resistivity of the solar cell and low efficiency. Usual strategy is to increase charge carrier concentration by positive doping. In terms of chemistry this process can be understood as oxidation. Doping of organic materials is complicated task. Lots of very different materials were tested. Here we will overview the most popular and effective ones.

Talk about additives to the **Spiro-OMeTAD** would be the best to start from the **LiTFSI**. It is the most used dopant in perovskite solar cells. **LiTFSI** mechanism of action for some time was unclear. In 2013 [42] it was shown that LiTFSI in oxygen atmosphere stimulates oxidation of the HTM (**Figure 9**). Still questionable is the role of formed LiO_2, Li+ ions and unreacted **LiTFSI**.
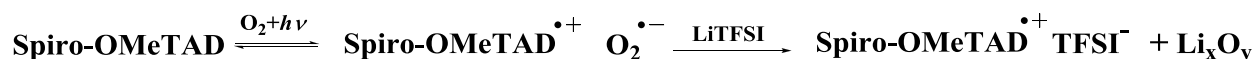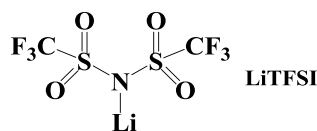
$$\text{Spiro-OMeTAD} \xrightarrow{O_2 + h\nu} \text{Spiro-OMeTAD}^{\bullet+} \; O_2^{\bullet-} \xrightarrow{\text{LiTFSI}} \text{Spiro-OMeTAD}^{\bullet+} \text{TFSI}^- + Li_xO_y$$

Figure 9. **LiTFSI** structure and proposed oxidation mechanism

Dependence on the environmental conditions (air oxygen) makes fabrication and encapsulation process very complicated, as it is unclear how to perform exposure to the oxygen (time, concentration etc.). Other drawback is that unreacted **LiTFSI** is strongly hygroscopic and provides to the moisture pathways to the perovskite surface [29].

In 2014 **AgTFSI** was tested as an alternative to **LiTFSI**. In this case oxidation occurs in the absence of O_2 (**Figure 10**) and better long-term stability can be achieved [43].

$$\text{Spiro-OMeTAD} \xrightarrow{\text{AgTFSI}} \text{Spiro-OMeTAD}^{\bullet+} \text{TFSI}^- + Ag$$

Figure 10. Oxidation with **AgTFSI**

In the same year in the group of prof. M. McGehee oxidation by AgTFSI were performed in solvent and Ag was consequentially removed from the final product. Dication salt with two TFSI⁻ counteranions (**Spiro(TFSI)₂**) were isolated and used as a dopant, making lithium free solar cells [41]. Earlier attempts to use oxidized **Spiro-OMeTAD** were unsuccessful due to the low solubility of the obtained salts [34]. TFSI⁻ is a weakly coordinating anion providing stability of the oxidized **Spiro-OMeTAD** and good solubility in organic solvents.

10

Another widely used strategy to oxidize **Spiro-OMeTAD** is to use cobalt complexes (e.g. tris(2-(1*H*-pyrazol-1-yl)pyridine)cobalt(III) (**FK102**) **Figure 11**). They are one electron oxidants and are suitable for the oxidation of the **Spiro-OMeTAD**. As oxygen is not required, generally better reproducibility is obtained. Usually this compounds are used in a combination with **LiTFSI** [44].
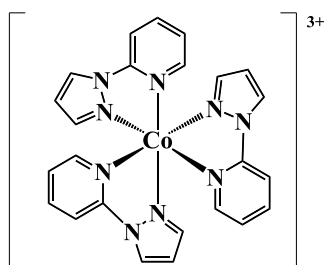

Figure 11. Cobalt complex **FK102**

Not only oxidative additives are used. In all devices with **Spiro-OMeTAD** 4-*tert*-butylpiridine (*t***BP**) is used. For the first time it was used in 1993 for DSSC. Dipping TiO$_2$ electrode into *t***BP** and addition of the small amount to the liquid electrolyte enhanced performance [45]. Lately on this material was transferred to the ssDSSC and then to perovskite solar cells. Action mechanism is still unclear. One of the possible effects is reduction of the trap states at the perovskite boundaries [46].

2.4.   Alternatives to the Spiro-OMeTAD

As mentioned above high HTM price is one of the unsolved problems. During the last few years, a number of various charge transporting materials were synthesized and investigated for the application in perovskite solar cells. Here we will review some classes of the HTM's. In all cases performance of the standard cell (prepared under the same conditions with **Spiro-OMeTAD** as a HTM) will be showed in brackets.
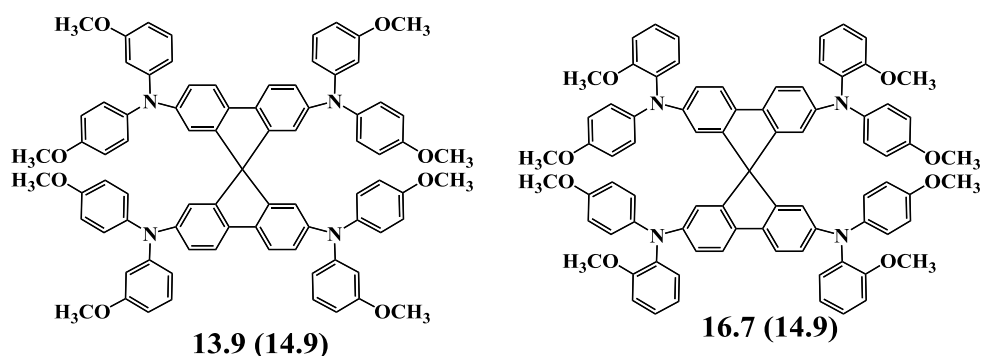
2.4.1. Spiro-OMeTAD like HTM's

Figure 12. **Spiro-OMeTAD** type compounds

In order to investigate influence of the methoxy group position three **Spiro-OMeTAD** isomers were synthesized and tested by S. I. Seok *et al*. [47]. Best result was obtained for the molecule with ortho substituent (**Figure 12**). This material have a highest LUMO value, therefore serves as a better electron blocking layer between Au electrode and perovskite. These results give us some insight on the desired properties of the molecule, but no improvement on the final product price is achieved.

2.4.2. Pyrene-based HTM's
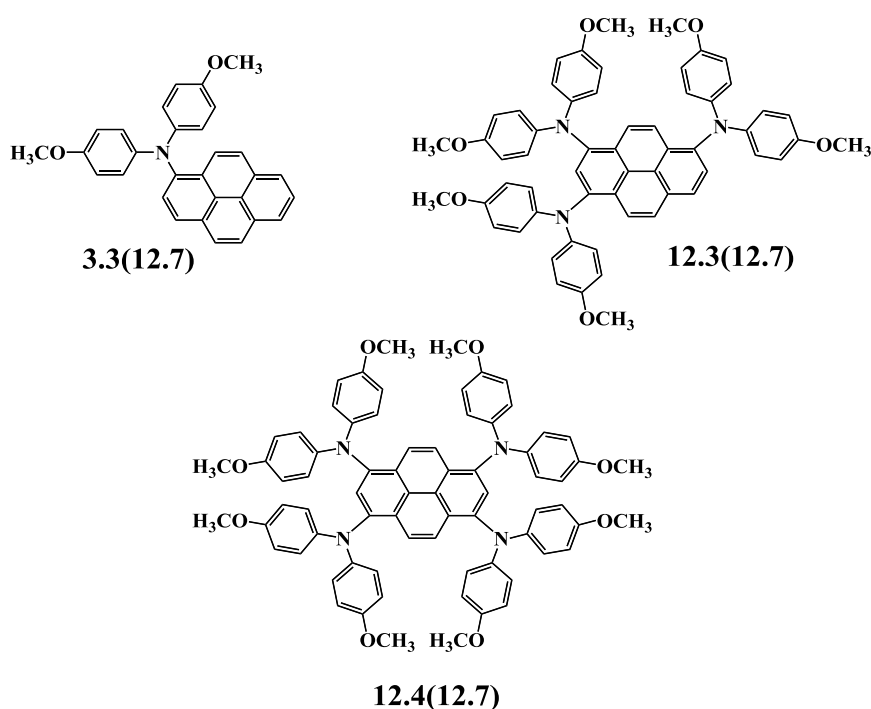
Figure 13. Pyrene-based HTM's

Also much simpler synthetic route was presented by the same authors [48]. It avoids complicated 9,9'-spirobifluorene core synthesis and uses as a starting material bromo-substituted pyrene. Three representatives were synthesized by the Buchwald−Hartwig amination reaction with one, three and four dimethoxy-diphenylamino fragments. Overall good results were

achieved with two of the synthesized HTM's (12.3 and 12.4 with the control 12.7). Some small drawbacks of these compounds are absorption in the visible light range (low LUMO), crystalline state and reducing in solubility with an increase in the number of di-*p*-methoxyphenylamino substituents.
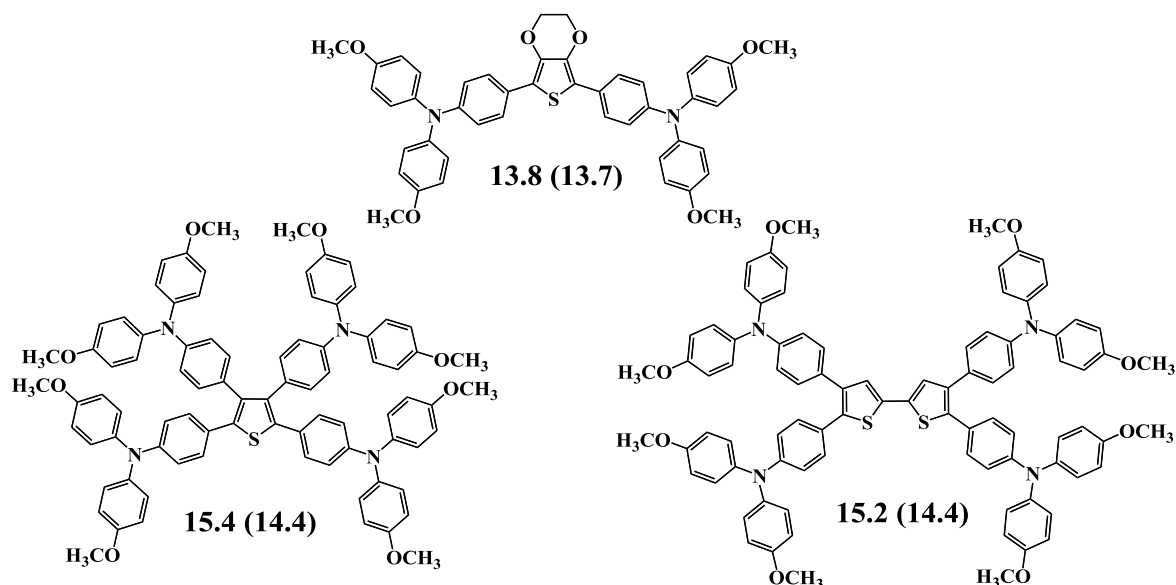
2.4.3. Thiophene-based HTM's

Figure 14. Thiophene-based HTM's

Other way to change 9,9'-spirobifluorene was proposed by S.G. Mhaisalkar and A.C. Grimsdale *et al.*. They developed a simpler small molecule HTM incorporating 3,4-ethylenedioxythiophene (**EDOT**) as a core [49]. Synthetic route includes bromination of the **EDOT** and a consequent Suzuki cross-coupling with {4-[bis(4-methoxyphenyl) amino]phenyl}boronic acid. As **EDOT** itself is also relatively high in price, thiophene and bithiophene were used for the similar synthetis purposes [50] (**Figure 14**).

These compounds after doping optimization showed slightly better performance in comparison to the **Spiro-OMeTAD**.
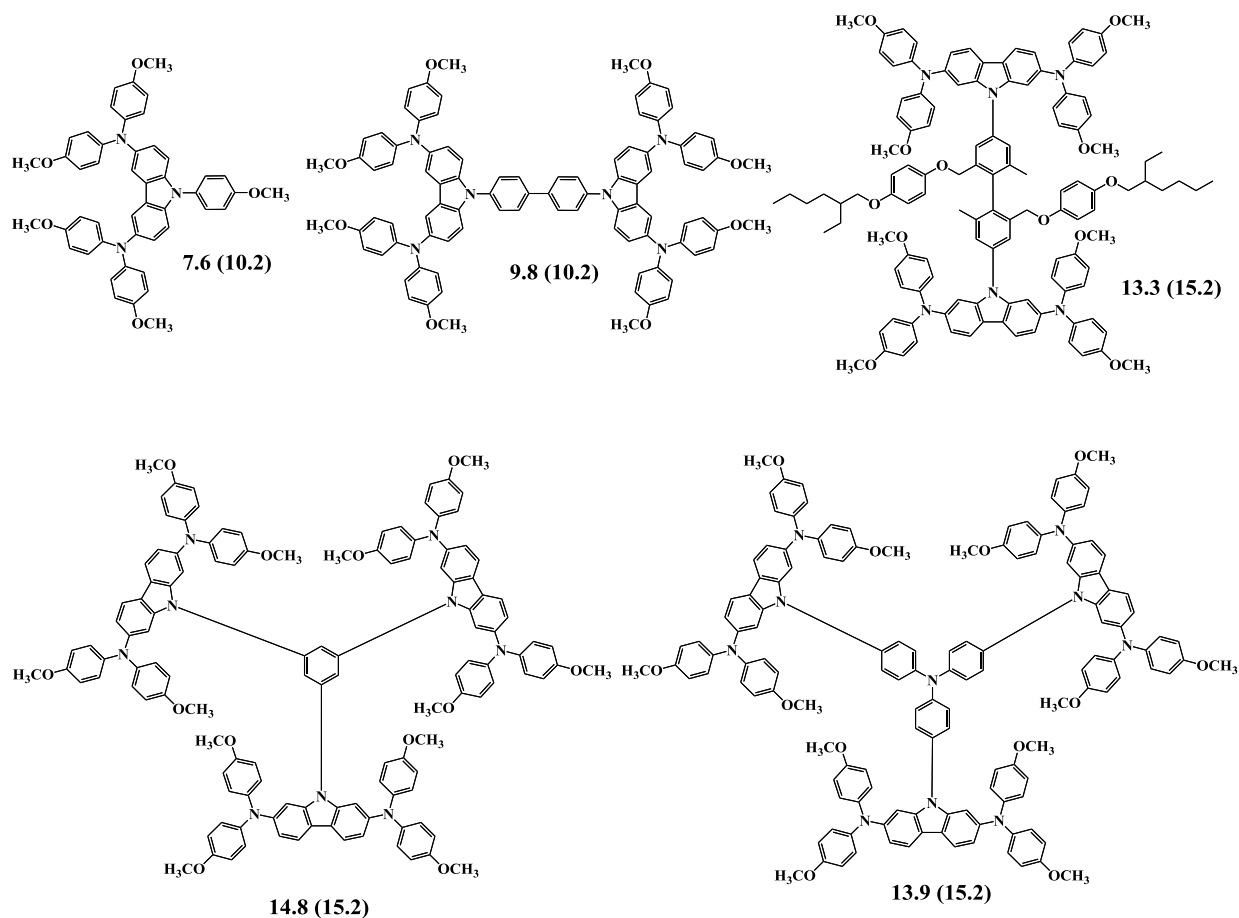
2.4.4. Carbazole-based HTM's

Figure 15. Carbazole-based HTM's

In 2014 L. Sun and co-workers synthesized and tested in perovskite solar cells two carbazole-based compounds [51] (**Figure 15** top left). One HTM shoved performance close to the **Spiro-OMeTAD**. Some questions are left, as control result was relatively low (only ~10%) so performance in the better cells is still unclear. Also three more molecules with branched structure were synthesized in the same year [52]. Instead of 3,6-substitued carbazole 2,7-dibromocarbazole, linked through phenylene, diphenylene or triphenylamine core, were used. Efficiencies for these HTM's exceeded 13%. The best value was 14.79%.
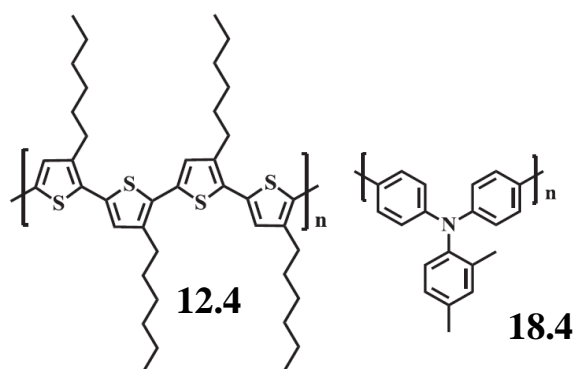
2.4.5. Polymers

Figure 16. **P3HT** and **PTAA**

Other widely used class of materials is conducting polymers. Among the first tested materials were poly(3-hexylthiophene-2,5-diyl) (**P3HT**). After optimization of layer formation parameters 9% efficiency was achieved [53]. In 2014 by using **LiTFSI** doping efficiency increased up to 12.4%, mostly due to increase of the conductivity [54]**.**

Lately on it was shown that triphenylamine-based polymer **PTAA** (Poly(triaryl amine)) overperform **P3HT** in an undoped state, showing 12% efficiency [55]. Lately on by changing some part (0.1-0.15) of the iodine in the perovskite to bromine incredible 18% efficiency was achieved [56].

2.4.6. Doping-free
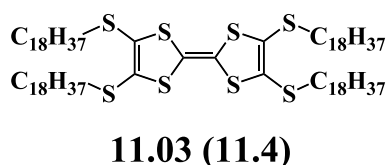

11.03 (11.4)

Figure 17. Tetrathiofulvalene-based dopant-free HTM

During the last year several dopant-free HTM's were reported to show high results in perovskite solar cells. These compounds have relatively high conductivity without oxidation. Due to a π-stacking such compounds have relatively high absorption in a visible light range. Still unclear is the absorption intensity influence on the overall performance. Another technical question is an assembly of the molecules. It was shown that heating at $65^{\circ}C$ for 24h. in argon atmosphere increase performance of the solar cell [57]. This can be attributed to the orientation of the molecules and formation of the more efficient π-stacking. As a consequence conductivity increases.

2.5. Synthesis of the new HTM's

In the beginning of the 21-st century novel trend appeared in the synthetic chemistry called "Click chemistry" [58]. The main idea is to adopt simple reactions for fast and versatile search of novel materials. To match this approach reaction should be modular, result in very high yields, generate non-toxic by-products, reaction conditions and product isolation has to be simple [59]. Originally it was proposed for the pharmacy, in order to speed-up process of determining structure-activity relationships and make scale-up process easier.
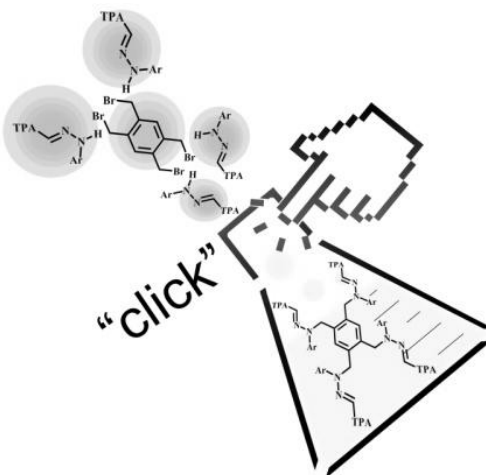
Figure 18 Proposed „Click" scheme for the synthesis of the novel HTM's

Same synthesis philosophy can be translated to the other fields of chemistry. In the Bachelor thesis [60] "Click" chemistry principles were adopted for the HTM's synthesis (**Figure 18**). Reaction between hydrazone with active hydrogen atom and aromatic linker with bromomethyl groups gave desired products in a high yields and with simple purification procedure.

2.6. Review conclusions

In a last two years perovskite solar cells have shown great promise as a cost-effective alternative to other solar technologies. Efficiencies have reached limit of the inorganic analogs and have potential to increase even more.

Literature review shoved that there are only very limited amount of hole transporting materials that are known to have good performance in the perovskite solar cells. Price of the most popular **Spiro-OMeTAD** is too high due to the long synthesis and cannot be reduced much. "Click" chemistry concept can help to overcome this problem. Hydrazones were used for the concept testing and structure influence on properties determination. Also HTM's with methoxydiphenylamine fragments were investigated in order to get materials more suitable to the existing doping procedure.

3. MATERIALS AND METHODS

Hydrazones **H(a-f)** and **DH(a,b)** were synthesized according to an earlier reported procedure [61] and after filtration and washing were directly used for the following synthesis. All other chemicals were purchased from Sigma-Aldrich and TCI Europe and used as received without further purification. Organic solvents were dried and purified by the standard methods [62]. Reactions were magnetically stirred and monitored by thin layer chromatography (TLC) with ALUGRAM SIL G/UV254 plates and developed with UV light. Silica gel (grade 9385, 230–400 mesh, 60 Å, Aldrich) was used for column chromatography. ^{1}H NMR (300 or 700 MHz field strength) spectra and ^{13}C NMR (75 or 176 MHz) were recorded with a Varian Unity Inova or Bruker Avance III 700. The chemical shifts, expressed in ppm, are reported relative to tetramethylsilane (TMS). UV-Vis spectra were recorded on Perkin Elmer Lambda 35 UV/Vis spectrometer. Melting points were determined for the crystalline materials on an Electrothermal MEL-TEMP capillary melting point apparatus and are uncorrected. Elemental analysis was performed with an Exeter Analytical CE-440 elemental analyzer, Model 440 C/H/N/. Differential scanning calorimetry (DSC) was performed on a Q10 calorimeter (TA Instruments) at a scan rate of 10 K min^{-1} in the nitrogen atmosphere. The glass transition temperatures for the synthesized compounds were determined during the second heating cycle.

UV/vis/NIR spectra were recorded on Shimadzu UV-3600 spectrometer. The mixture of **o-OMeCz** and AgTFSI (1, 2, 3 and 4 equivalents) in DCM (under argon atmosphere) was stirred overnight (or for one hour) at the room temperature. The solutions were filtered and diluted to the final concentration of the 10^{-4} M.

Molecular weight of the hydrazone polymers were determined by a gel permeation chromatography using GPC systems including Bischoff LAMBDA 1000 detector and GMH_{HR}-M columns. THF was used as an eluent, polystyrene standards were used for column system calibration.

Ionization potential (I_p) of the solid state materials was measured by the electron photoemission in air method [63] from the layers of the synthesized HTM's. Hole drift mobility (μ) has been measured by xerographic time of flight method (XTOF) [64]. I_p and μ were measured at the Departament of Solid State Electronics, Vilnius University by dr. V. Gaidelis and dr. V. Jankauskas.

Preliminary tests of the performance in solar cells with **2H3** and **PH2** were performed at the Photovoltaic and Optoelectronic Device Group, University of Oxford, United Kingdom by dr. James Ball.

Solar cells with twin molecules (**(o,m,p)-(O)MeCz**) were fabricated following a one-step anti-solvent approach [65] at the Laboratory for Photonics and Interfaces, École Polytechnique Fédérale de Lausanne, Switzerland by Paul Gratia. HTM's were spin-coated from a chlorobenzene solution (30mmol in 400µl,) using **LiTFSI** (3.5µl from a 520mg/ml stock solution in acetonitrile), **tBP** (5.8µl) and **FK102** (freshly prepared [44], 10mol%, 4.4µl from a 40mg/ml stock solution). **Spiro-OMeTAD** were spin-coated from a chlorobenzene solution (28.9mg in 400µl, 60mmol) using **LiTFSI** (7.0µl from a 520mg/ml stock solution in acetonitrile), tBP (11.5µl) and **FK102** (freshly prepared, 10mol%, 8.8µl from a 40mg/ml stock solution). The spin conditions for both of the compounds were: speed - 4000rpm, time – 20 s.

3.1. Synthesis of the branched hydrazones

Synthesis of the hydrazones **(2-4)H(a,b)** were described in the Bsc thesis [60].

3.1.1. Synthesis of the dihydrazones

General procedure:

To a solution of 1,3-bis(bromomethyl)benzene (1 eq.) in acetone (12ml/mmol) 2.5 eq of HYDRAZONE was added. The mixture was stirred at reflux for 1 h, followed by addition of 5.8 eq. powdered KOH. Completeness of the reaction was controlled by TLC. Product purification PROCEDURE is specified in more details for each compound.

2Hc: *1,3-bis{1-phenyl-2-[4-(bis(9,9-dimethyl-9H-fluoren-2-yl)amino)benzyliden] hydrazinmethyl}benzene*
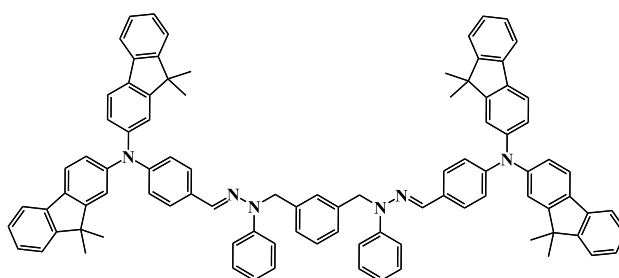
HYDRAZONE: 4-(bis(9,9-dimethyl-9*H*-fluoren-2-yl)amino)benzaldehyde *N*-phenyl-hydrazone (0.87 g 1.47mmol)

TLC: toluene:*n*-hexane; 10:15 v:v

PROCEDURE: the reaction mixture was treated with ethyl acetate and washed with distilled H$_2$O. The organic layer was dried over anhydrous Na$_2$SO$_4$, filtered and the solvents

were removed. The residue was purified by column chromatography (eluent toluene:*n*-hexane; 10:15 v:v)

Yield - 0.60 g (79 %)*;* m.p. 195°C.

^{1}H NMR (300 MHz, CDCl$_3$) δ 7.63 – 6.88 (m, 52H), 5.14 (s, 4H), 1.38 (s, 24H).

^{13}C NMR (75 MHz, CDCl$_3$) δ 155.17, 153.63, 147.96, 147.91, 147.19, 139.05, 137.06, 134.40, 132.55, 130.81, 129.94, 129.32, 129.16, 127.24, 127.13, 126.63, 125.30, 123.97, 123.83, 123.36, 122.61, 120.76, 119.57, 118.77, 114.82, 50.54, 46.95, 27.17.

Anal. calcd for C$_{94}$H$_{80}$N$_6$: C, 87.27; H, 6.23; N, 6.50; found: C, 87.15; H, 6.25; N,6.44.

3.1.2. Synthesis of the trihydrazones

General procedure:

To a solution of 2,4,6-tris(bromomethyl)mesitylene (1 eq.) in acetone (20ml/mmol) 3.5 eq of HYDRAZONE was added. The mixture was stirred at reflux for 1.5 h, followed by addition of 8 eq. powdered KOH. Completeness of the reaction was controlled by TLC. Product purification PROCEDURE is specified in more details after each compound.

3Hc: *2,4,6-tris{1-phenyl-2-[4-(4,4'-dimethyldiphenylamino)benzyliden]hydrazinmethyl} 1,3,5-trimethylbenzene*
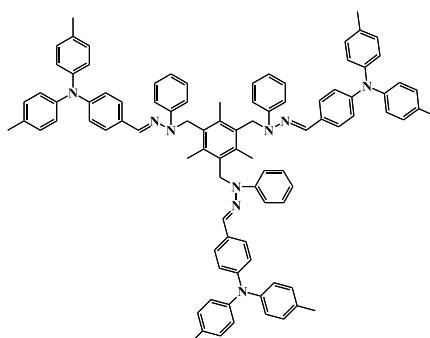
HYDRAZONE: 4-(4,4'-dimethyldiphenylamino)benzaldehyde *N*-phenyl-hydrazone (1.1g 2.8mmol)

TLC: toluene:methanole:*n*-hexane, 3:1:21 v:v:v

PROCEDURE: the reaction mixture was treated with chloroform and washed with distilled H$_2$O. The organic layer was dried over anhydrous Na$_2$SO$_4$, filtered and the solvents were

removed. The residue was purified by column chromatography (acetone:diethyl ether:*n*-hexane, 1:5:19 v:v:v)

The yield was 0.58 g (53 %)

1H-NMR (300MHz, CDCl3), δ 7.33-6.87 (m, 54H); 4.77 (s, 6H); 2.29 (s, 18H); 2,23 (s, 9H)

^{13}C NMR (75 MHz, CDCl$_3$) δ 148.03, 147.31, 145.20, 137.43, 136.42, 132.65, 132.33, 129.97, 129.01, 126.98, 124.73, 124.12, 123.18, 122.48, 52.91, 20.95, 16.79.

Anal. calcd for C$_{93}$H$_{87}$N$_9$: C, 83.94; H, 6.59; N, 9.47; found: C, 83.77; H, 6.52; N, 9.44.

3Hd: *2,4,6-tris{1-phenyl-2-[4-(diphenylamino)benzyliden]hydrazin-2-methyl}1,3,5-trimethylbenzene*
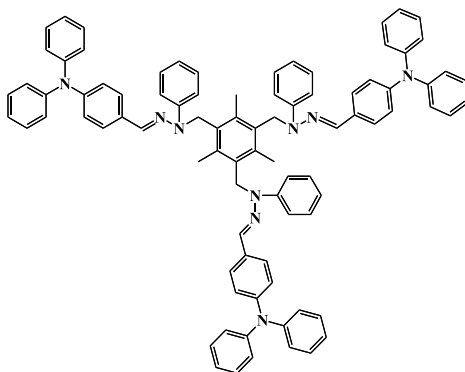
HYDRAZONE: 4-(diphenylamino)benzaldehyde *N*-phenylhydrazone (1.5g 4.1mmol)

TLC: acetone:*n*-hexane, 3:22 v:v

PROCEDURE: the reaction mixture was treated with dichloromethane and washed with distilled H$_2$O. The organic layer was dried over anhydrous Na$_2$SO$_4$, filtered and the solvents were removed. The residue was purified by column chromatography (eluent acetone:*n*-hexane, 3:22 v:v)

The yield was 0.81g (55 %)

^{1}H-NMR (300MHz, CDCl$_3$), δ 7.37-6.91 (m, 60H); 4.80 (s, 6H); 2.24 (s, 9H)

^{13}C NMR (75 MHz, CDCl$_3$) δ 147.65, 147.54, 147.10, 137.44, 135.63, 132.34, 130.92, 129.35, 129.07, 127.04, 124.48, 124.33, 123.69, 123.37, 123.02, 52.98, 16.83.

Anal. calcd for $C_{87}H_{75}N_9$: C, 83.82; H, 6.06; N, 10.11; found, %: C,83.80; H, 5.99; N, 10.01.

3.1.3. Synthesis of the tetrahydrazones

General procedure:

To a solution of 1,2,4,5-tetrakis(bromomethyl)benzene (1 eq.) in acetone (34ml/mmol) 4.5 eq of <u>HYDRAZONE</u> was added. The mixture was stirred at reflux for 1.5 h, followed by addition of 10.4 eq. powdered KOH. Completeness of the reaction was controlled by <u>TLC</u>. Product purification <u>PROCEDURE</u> is specified in more details after each compound.

4Hc: *1,2,4,5-tetrakis{1-phenyl-2-[4-(4,4'-dimethyldiphenylamino)benzyliden] hydrazinmethyl}benzene*
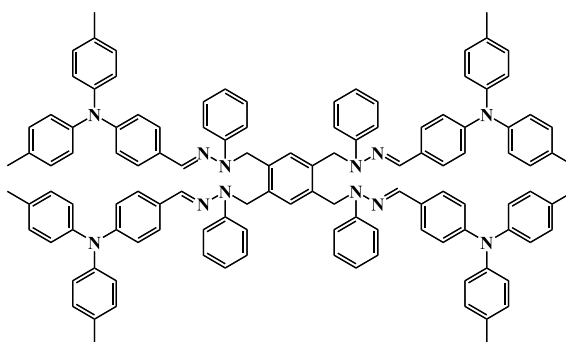
<u>HYDRAZONE</u>: 4-(4,4'-dimethyldiphenylamino)benzaldehyde *N*-phenylhydrazone (0.56 g 1.4mmol)

<u>TLC</u>: ethyl acetate:diethyl ether:*n*-hexane, 1:1:20 v:v:v

<u>PROCEDURE</u>: obtained solid was filtered and washed with water (until neutral reaction) and 2-propanole.

The yield was 0.27 g (51 %); m.p. 143-144°C (recrystallized from toluene:acetone, 1:1 v:v)

^{1}H-NMR (300MHz, CDCl$_3$), δ 7.28-6.77 (m, 74H); 5.01 (s, 8H); 2.29 (s, 24H)

^{13}C NMR (75 MHz, DMSO) δ 148.17, 147.26, 145.23, 133.39, 132.78, 132.72, 130.02, 129.75, 129.18, 127.61, 127.25, 124.75, 122.48, 121.24, 116.24, 49.09, 20.96.

Anal. calcd for $C_{118}H_{106}N_{12}$: C, 83.75; H, 6.31; N, 9.93; found: C, 83.70; H, 6.33; N,9.87 .

4Hd: *1,2,4,5-tetrakis{1-phenyl-2-[4-(benzyl(ethyl)amino)benzyliden]hydrazinmethyl}* *benzene*
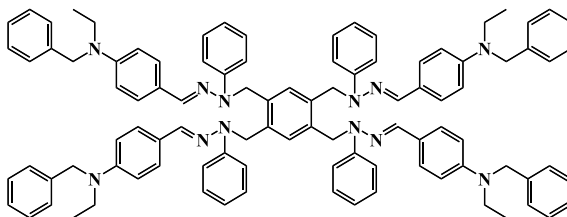
HYDRAZONE: 4-(benzyl(ethyl)amino)benzaldehyde *N*-phenyl-hydrazone (2.2 g 6.68 mmol)

TLC: acetone:*n*-hexane, 5:20 v:v

PROCEDURE: obtained solid was filtered and washed with water (until neutral reaction) and diethyl ether.

The yield was 1.54 g (72 %); m.p. 178°C (recrystallized from toluene)

^{1}H-NMR (300MHz, DMSO), δ 7.39-6.96 (m, 48H); 6.72-6.54 (m, 14H); 5.15 (s, 8H); 4.56 (s, 8H); 3.58-3.42 (m, 8H); 1.16 (t, J=6.8Hz, 12H)

13C NMR (75 MHz, DMSO) δ 147.69, 147.25, 139.14, 133.89, 133.86, 132.11, 128.68, 128.43, 127.40, 126.67, 126.45, 123.87, 119.29, 114.35, 111.55, 52.97, 46.12, 44.94, 12.19.

Anal. calcd for $C_{98}H_{98}N_{12}$: C, 81.52; H, 6.84; N, 11.64; found: C, 81.36; H, 6.81; N, 11.69.

4He: *1,2,4,5-tetrakis{1-[4-methylphenyl]-2-[4-(4-methyldiphenylamino)benzyliden]* *hydrazinmethyl}benzene*
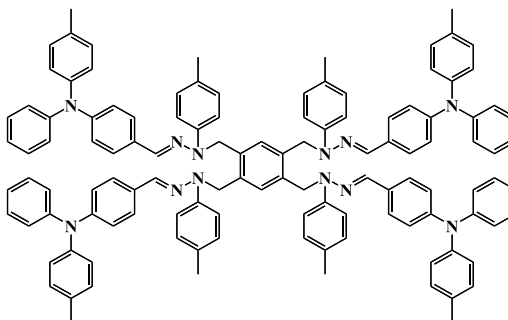
HYDRAZONE: 4-(4-methyldiphenylamino)benzaldehyde *N*-(4-methylphenyl)-hydrazone (0.8 g 2.04 mmol)

TLC: toluene:*n*-hexane, 15:10 v:v

PROCEDURE: the reaction mixture was treated with chloroform and washed with distilled H_2O. The organic layer was dried over anhydrous Na_2SO_4, filtered and the solvents were

removed. The residue was purified by column chromatography (eluent acetone:*n*-hexane, 5:20 v:v)

The yield was 0.40 g (52 %); amorphous solid.

^{1}H-NMR (300MHz, CDCl$_3$), δ 7.28-6.85 (m, 74H); 4.98 (s, 8H); 2.29 (s, 12H); 2.21 (s, 12H)

^{13}C NMR (75 MHz, CDCl$_3$) δ 147.78, 145.00, 133.05, 132.94, 132.73, 130.78, 130.55, 130.42, 130.08, 129.76, 129.28, 127.09, 126.22, 125.12, 123.97, 123.05, 122.65, 118.87, 116.86, 49.92, 29.84, 20.98.

Anal. calcd for C$_{118}$H$_{106}$N$_{12}$: C, 83.75; H, 6.31; N, 9.93; found: C, 83.71; H, 6.20; N, 9.85.

4Hf: *1,2,4,5-tetrakis{1-[3-methylphenyl]-2-[4-(4,4'-dimethyldiphenylamino)benzyliden] hydrazinmethyl}benzene*
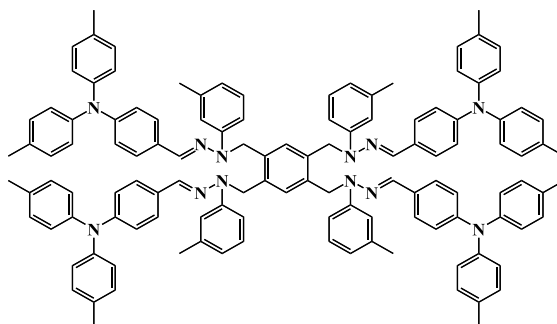
HYDRAZONE: 4-(4,4'-dimethyldiphenylamino)benzaldehyde   *N*-(3-methylphenyl)-hydrazone (0.48 g 1.2mmol)

TLC: toluene:*n*-hexane, 20:5 v:v

PROCEDURE: the reaction mixture was treated with chloroform and washed with distilled H$_2$O. The organic layer was dried over anhydrous Na$_2$SO$_4$, filtered and the solvents were removed. The residue was purified by column chromatography (eluent toluene:*n*-hexane, 10:15 v:v)

The yield was 0.26 g (61 %); m.p. 66°C

^{1}H-NMR (300MHz, CDCl$_3$), δ 7.28-6.83 (m, 66H); 6.64 (d, J=7.4Hz, 4H); 5.00 (s, 8H); 2.28 (s, 24H); 2.21 (s, 12H)

^{13}C NMR (75 MHz, CDCl$_3$) δ 148.06, 147.36, 145.22, 138.93, 133.10, 132.83, 132.67, 130.00, 129.87, 128.98, 128.36, 127.17, 124.71, 122.48, 122.16, 116.88, 113.22, 49.28, 21.93, 20.95.

Anal. calcd for $C_{122}H_{114}N_{12}$: C, 83.81; H, 6.57; N, 9.61; found: C, 83.72; H, 6.59; N, 9.54.

3.2. Synthesis of the polyhydrazones

General procedure:

To a solution of 1,3-bis(bromomethyl)benzene (0.4 g, 1.5 mmol) in THF (7 ml) 1.5mmol of <u>HYDRAZONE</u> was added. The mixture was stirred at reflux for 1 h, followed by addition of 5.8 eq. powdered KOH. Completeness of the reaction was controlled by TLC (acetone:*n*-hexane, 1:4). Obtained solid was filtered and washed with water (until neutral reaction) and methanol. The crude product was purified by column chromatography using 1:2 v/v acetone/*n*-hexane as a starting eluent and THF at the end. The obtained product was precipitated from 20% solution in THF into 15-fold excess of methanol. The precipitate was filtered off and washed with methanol to collect final compound.

PHa: *Poly{4,4'-[(4-methoxyphenyl)azanediyl]dibenzaldehyde bis(N-phenylhydrazone)-alt-1,3-bis(bromomethyl)benzene}*
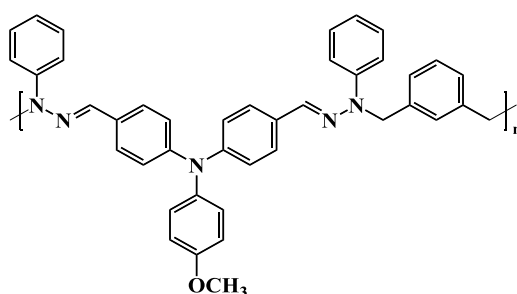
<u>HYDRAZONE</u>: 4,4'-[(4-methoxyphenyl)azanediyl]dibenzaldehyde bis(*N*-phenylhydrazone) 0.8g

Yield: 0.83g (86.5%)

GPC: $M_{\mathrm{w}} = 30910$, $M_{\mathrm{n}} = 12151$.

Anal. calcd for $(C_{41}H_{35}N_5O)_n$: C, 80.23; H, 5.75; N, 11.41; found, %: C,80.19; H, 5.76; N, 11.40.

^{1}H NMR (700 MHz, DMSO) δ 7.53 – 6.57 (m, 28H), 5.28 – 4.95 (m, 4H), 3.73 – 3.54 (m, 3H)

PHb: *Poly{ 4,4'-[(4-methoxy-3-methylphenyl)azanediyl]dibenzaldehyde bis(N-phenylhydrazone)-alt-1,3-bis(bromomethyl)benzene}*
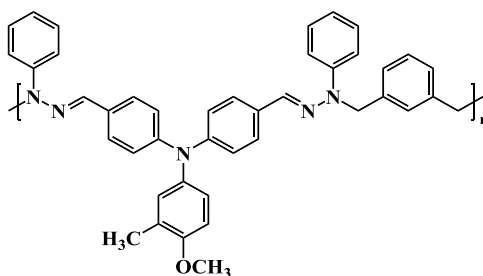
HYDRAZONE: 4,4'-[(4-methoxy-3-methylphenyl)azanediyl]dibenzaldehyde bis(*N*-phenylhydrazone) 0.8g

Yield: 0.75g (78.5%)

GPC: $M_w = 16485$, $M_n = 8958$.

Anal. calcd for $(C_{42}H_{37}N_5O)_n$: C, 80.35; H, 5.94; N, 11.16; found, %: C,80.30; H, 5.93; N, 11.17.

^{1}H NMR (700 MHz, DMSO) δ 7.53 – 6.61 (m, 27H), 5.37 – 4.97 (m, 4H), 3.76 – 3.51 (m, 3H), 2.05 – 1.85 (m, 3H).

3.3. Synthesis of the diphenylamine substituted carbazole twin molecules

3.3.1. Intermediate compounds

General procedure:

A mixture of 3,6-dibromo-9*H*-carbazole (1.30 g, 4 mmol) and <u>DIBROMOXYLENE</u> (0.53 g, 2 mmol) was dissolved in 15 ml of THF and 0.80 g (0.012 mol) of 85% powdered potassium hydroxide was added in small portions during 2-3 minutes. The obtained mixture was vigorously stirred at room temperature for 10 min (TCL, acetone:hexane, 1:4). The product was filtered off and washed with water until neutral and three times with ethanol. Compound was dried in vacuum oven at 40°C for 24 hours and used in the next step without additional purification.

o-Cz: *1,2-Bis(3,6-dibromo-9H-carbazol-9-methyl)benzene*
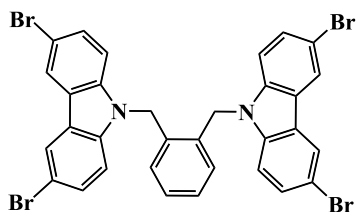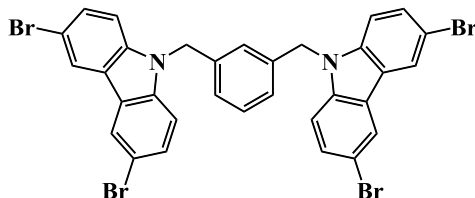

DIBROMOXYLENE: 1,2- bis(bromomethyl)benzene

Yield: 1.35 g, 89.7%, m.p. 317-319°C.

^{1}H NMR (700 MHz, DMSO) δ 8.60 (s, 4H), 7.67 (t, *J* = 5.8 Hz, 8H), 6.90 (dd, *J* = 5.6, 3.2 Hz, 2H), 6.00 (s, 4H), 5.97 − 5.94 (m, 2H).

^{13}C NMR (176 MHz, DMSO) δ 139.52, 133.99, 129.07, 127.00, 123.86, 123.74, 123.18, 112.07, 111.91, 43.23.

Anal. calcd for $C_{32}H_{20}Br_4N_2$: C, 51.10; H, 2.68; N, 3.72; found: C, 51.00; H, 2.59; N, 3.75.

m-Cz: *1,3-Bis(3,6-dibromo-9H-carbazol-9-methyl)benzene*

DIBROMOXYLENE: 1,3- bis(bromomethyl)benzene

Yield: 1.3 g, 86%, m.p. 255-256°C

^{1}H NMR (700 MHz, DMSO) δ 8.41 (d, *J* = 1.9 Hz, 4H), 7.45 (dd, *J* = 8.7, 2.0 Hz, 4H), 7.40 (d, *J* = 8.7 Hz, 4H), 7.18 (t, *J* = 7.7 Hz, 1H), 7.03 (dd, *J* = 7.7, 1.0 Hz, 2H), 6.63 (s, 1H), 5.52 (s, 4H).

^{13}C NMR (176 MHz, DMSO) δ 138.98, 137.56, 128.95, 128.76, 125.85, 124.64, 123.36, 122.95, 111.63, 111.54, 45.47.

Anal. calcd for $C_{32}H_{20}Br_4N_2$: C, 51.10; H, 2.68; N, 3.72; found: C, 50.96; H, 2.69; N, 3.70.

p-Cz:*1,4-Bis(3,6-dibromo-9H-carbazol-9-methyl)benzene*
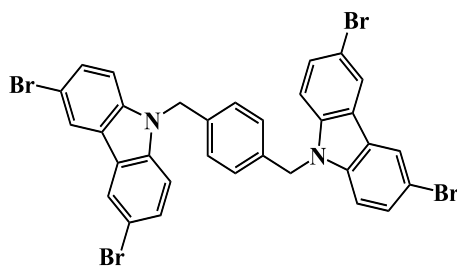
DIBROMOXYLENE: 1,4 - bis(bromomethyl)benzene

Yield: 1.37 g, 91.1%, m.p. 330-332°C.

^{1}H NMR (700 MHz, DMSO) δ 8.48 (d, *J* = 1.4 Hz, 4H), 7.59 − 7.54 (m, 8H), 7.01 (s, 4H), 5.60 (s, 4H).

^{13}C NMR (176 MHz, DMSO) δ 139.16, 136.40, 128.98, 126.92, 123.52, 123.09, 111.86, 111.63, 45.39.

Anal. calcd for $C_{32}H_{20}Br_4N_2$: C, 51.10; H, 2.68; N, 3.72; found: C, 51.01; H, 2.60; N, 3.73.

3.3.2. HTM's

General procedure:

A solution of INTERMIDIENT COMPOUND (1.13 g, 1.5 mmol), DIPHENYLAMINE (7.5 mmol) in anhydrous toluene (15 mL) was purged with argon for 20 minutes. Afterwards, palladium(II) acetate (6.7 mg, 0.03 mmol), tri-*tert*-butylphosphonium tetrafluoroborate (11.6 mg, 0.04 mmol) and sodium *tert*-butoxide (0.72 g, 7.5 mmol) were added and the solution was refluxed under argon atmosphere for 20 hours. After cooling to room temperature, reaction mixture was filtered through Celite. 50 mL of distilled water was added to the filtrate and extraction was done with ethyl acetate. The combined organic layer was dried over anhydrous Na_2SO_4, filtered and solvent evaporated. The crude product was purified by column chromatography using 1:3 v/v acetone/*n*-hexane as an eluent. The obtained product was precipitated from 20% solution in acetone into 15-fold excess of methanol. The precipitate was filtered off and washed with methanol to collect final compound.

o-MeCz: *1,2-Bis[3,6-(4,4-dimethyldiphenylamino)-9H-carbazol-9-methyl]benzene*
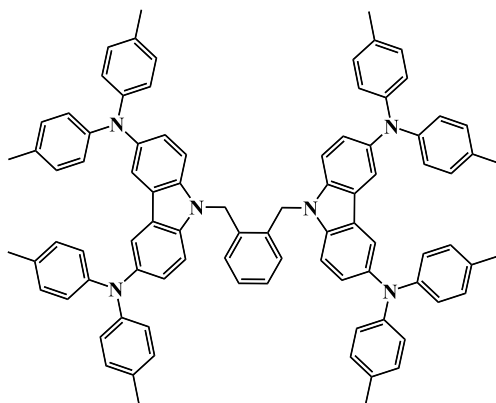
INTERMIDIENT COMPOUND: **o-Cz**

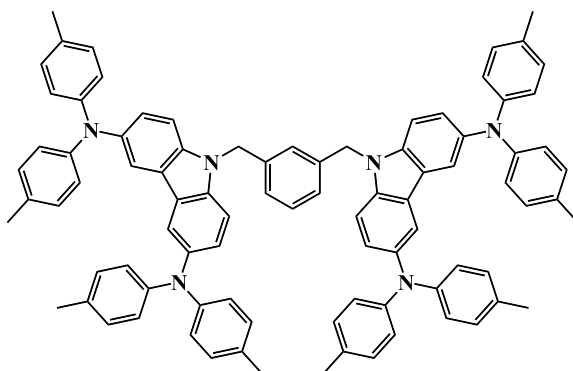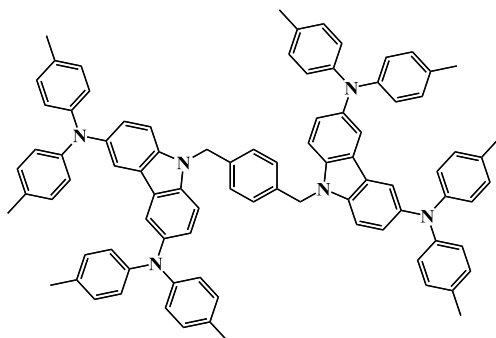DIPHENYLAMINE: 4,4'-dimethyldiphenylamine, 1.48 g

Yield: 1.27 g, 69 %

^{1}H NMR (700 MHz, DMSO) δ 7.64 – 6.81 (m, 48H), 5.98 (s, 4H), 2.18 (s, 24H)

^{13}C NMR (176 MHz, DMSO) δ 151.46, 139.19, 129.71, 129.51, 128.03, 125.86, 124.91, 122.25, 122.10, 120.47, 119.23, 116.68, 109.69, 43.08, 20.24

Anal. calcd for $C_{88}H_{76}N_6$: C, 86.81; H, 6.29; N, 6.90; found: C, 86.69; H, 6.23; N, 6.85.

m-MeCz: *1,3-Bis[3,6-(4,4-dimethyldiphenylamino)-9H-carbazol-9-methyl]benzene*

INTERMIDIENT COMPOUND: **m-Cz**

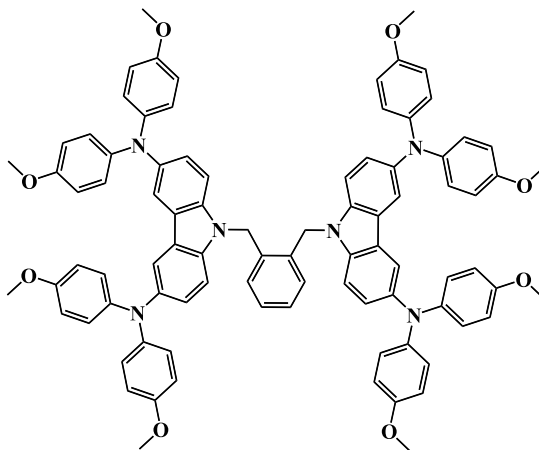DIPHENYLAMINE: 4,4'-dimethyldiphenylamine, 1.48 g

Yield: 1.42 g, 78%

^{1}H NMR (700 MHz, DMSO) δ 7.77 (s, 4H), 7.53 (d, J = 8.4 Hz, 4H), 7.46 (s, 1H), 7.29 – 7.17 (m, 3H), 7.07 – 6.95 (m, 20H), 6.78 (d, J = 7.7 Hz, 16H), 5.53 (s, 4H), 2.19 (s, 24H)

^{13}C NMR (176 MHz, DMSO) δ 145.92, 139.44, 137.64, 132.08, 130.20, 129.64, 129.45, 126.72, 126.47, 125.44, 122.88, 122.02, 118.32, 110.68, 45.90, 20.23

Anal. calcd for $C_{88}H_{76}N_6$: C, 86.81; H, 6.29; N, 6.90; found: C, 86.72; H, 6.28; N, 6.88.

p-MeCz: *1,4-Bis[3,6-(4,4-dimethyldiphenylamino)-9H-carbazol-9-methyl]benzene*

INTERMIDIENT COMPOUND: **p-Cz**

DIPHENYLAMINE: 4,4'-dimethyldiphenylamine, 1.48 g

Yield: 1.26 g, 69 %

^{1}H NMR (700 MHz, DMSO) δ 7.75 (s, 4H), 7.45 (s, 4H), 7.17 − 6.70 (m, 40H), 5.48 (s, 4H), 2.18 (s, 24H).

^{13}C NMR (176 MHz, DMSO) δ 145.91, 139.45, 137.68, 136.86, 130.18, 129.62, 127.08, 125.40, 122.85, 122.03, 118.29, 110.52, 45.49, 20.22.

Anal. calcd for $C_{88}H_{76}N_6$: C, 86.81; H, 6.29; N, 6.90; found: C, 86.67; H, 6.21; N, 6.86.

o-OMeCz: *1,2-Bis[3,6-(4,4-dimethoxydiphenylamino)-9H-carbazol-9-methyl]benzene*

INTERMIDIENT COMPOUND: **o-Cz**

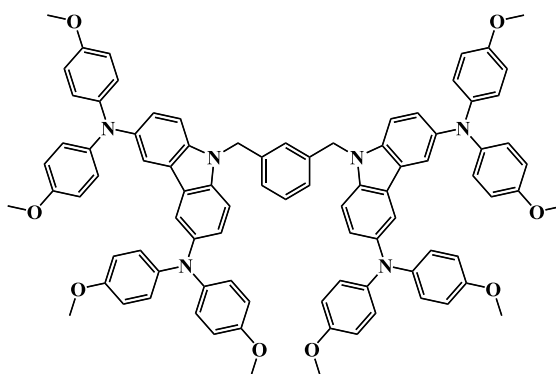DIPHENYLAMINE: 4,4'-dimethoxydiphenylamine, 1.72 g

Yield: 1.35 g, 67%

^{1}H NMR (700 MHz, DMSO) δ 7.71 (d, J = 1.5 Hz, 4H), 7.39 (d, J = 8.8 Hz, 4H), 7.08 (dd, J = 8.7, 1.4 Hz, 4H), 7.02 (dd, J = 5.1, 3.4 Hz, 2H), 6.85 (d, J = 8.9 Hz, 16H), 6.78 (d, J = 9.0 Hz, 16H), 6.48 – 6.44 (m, 2H), 5.80 (s, 4H), 3.66 (s, 24H)

^{13}C NMR (176 MHz, DMSO) δ 154.23, 142.01, 140.48, 137.47, 134.72, 129.43, 124.30, 123.81, 122.88, 116.74, 114.63, 113.83, 110.53, 55.13, 43.53

Anal. calcd for $C_{88}H_{76}N_6O_8$: C, 78.55; H, 5.69; N, 6.25; found: C, 78.50; H, 5.66; N, 6.22.

m-OMeCz: *1,3-Bis[3,6-(4,4-dimethoxydiphenylamino)-9H-carbazol-9-methyl]benzene*

INTERMIDIENT COMPOUND: **m-Cz**

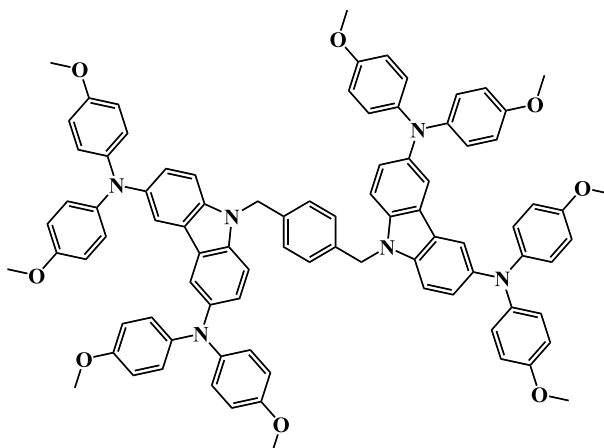DIPHENYLAMINE: 4,4'-dimethoxydiphenylamine, 1.72 g

Yield: 1.75 g, 87%

^{1}H NMR (700 MHz, DMSO) δ 7.66 (d, J = 1.8 Hz, 4H), 7.50 (d, J = 8.8 Hz, 4H), 7.46 (s, 1H), 7.23 (t, J = 7.6 Hz, 1H), 7.14 (d, J = 7.6 Hz, 2H), 7.04 (dd, J = 8.7, 1.9 Hz, 4H), 6.84 (d, J = 9.0 Hz, 16H), 6.78 (d, J = 9.0 Hz, 16H), 5.51 (s, 4H), 3.68 (s, 24H)

^{13}C NMR (176 MHz, DMSO) δ 154.17, 142.03, 140.24, 138.21, 137.15, 129.04, 126.76, 126.30, 124.37, 123.72, 122.76, 116.73, 114.60, 110.54, 55.07, 45.86

Anal. calcd for $C_{88}H_{76}N_6O_8$: C, 78.55; H, 5.69; N, 6.25; found: C, 78.48; H, 5.67; N, 6.21.

p-OMeCz: *1,4-Bis[3,6-(4,4-dimethoxydiphenylamino)-9H-carbazol-9-methyl]benzene*

INTERMIDIENT COMPOUND: **p-Cz**

DIPHENYLAMINE: 4,4'-dimethoxydiphenylamine, 1.72 g

Yield: 1.33 g, 66%

^{1}H NMR (700 MHz, DMSO) δ 7.56 (s, 4H), 7.27 (s, 4H), 7.00 – 6.90 (m, 8H), 6.76 (d, *J* = 8.9 Hz, 16H), 6.70 (d, *J* = 9.0 Hz, 16H), 5.35 (s, 4H), 3.62 (s, 24H)

^{13}C NMR (176 MHz, DMSO) δ 154.61, 142.50, 140.72, 137.64, 137.25, 127.38, 124.80, 124.22, 123.19, 117.15, 115.03, 110.73, 55.57, 45.89

Anal. calcd for $C_{88}H_{76}N_6O_8$: C, 78.55; H, 5.69; N, 6.25; found: C, 78.51; H, 5.62; N, 6.22

4. RESULTS AND DISCUSSIONS

4.1. Branched hydrazone HTM's

Materials with hydrazone (>C=N–N<) functional groups are widely used in a different areas, e.g. medicine [66], organic synthesis [67], as a molecular switches [68]. One of the important application field – HTM's in different electronic devices [69]. Suitable hole drift mobilities in a combination with a relatively simple synthesis makes them attractive for industrial uses. On the other hand high cristallinity is often a limiting factor because of the poor long-term stability of amorphous HTM layers. It enforces to use materials dispersed in polymer binder or attached to the polymer chain as a side group [70]. Inactive components reduce concentration of hydrazone moieties and consequently decrease overall performance. That is why new material structures are needed. Usual strategies are synthesis of dendrimeric or branched structures. These methods afford a better photophysical and morphological properties. However they have two main disadvantages: complicated synthesis process with low yields and high environmental impact [71, 72]. "Click" chemistry possibilities for the HTM synthesis were investigated in a more details on the hydrazone example.

4.1.1. Synthesis

Synthesis of the branched hydrazones was made by the two step synthesis (**Figure 20**). Intermediate hydrazones **H(a-f)** with various electron donor groups were freshly prepared by a simple reaction of aromatic aldehyde with phenylhydrazine [61] and after filtration and washing with hexane were directly used for the following synthesis.
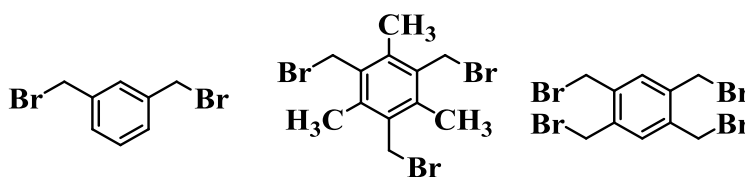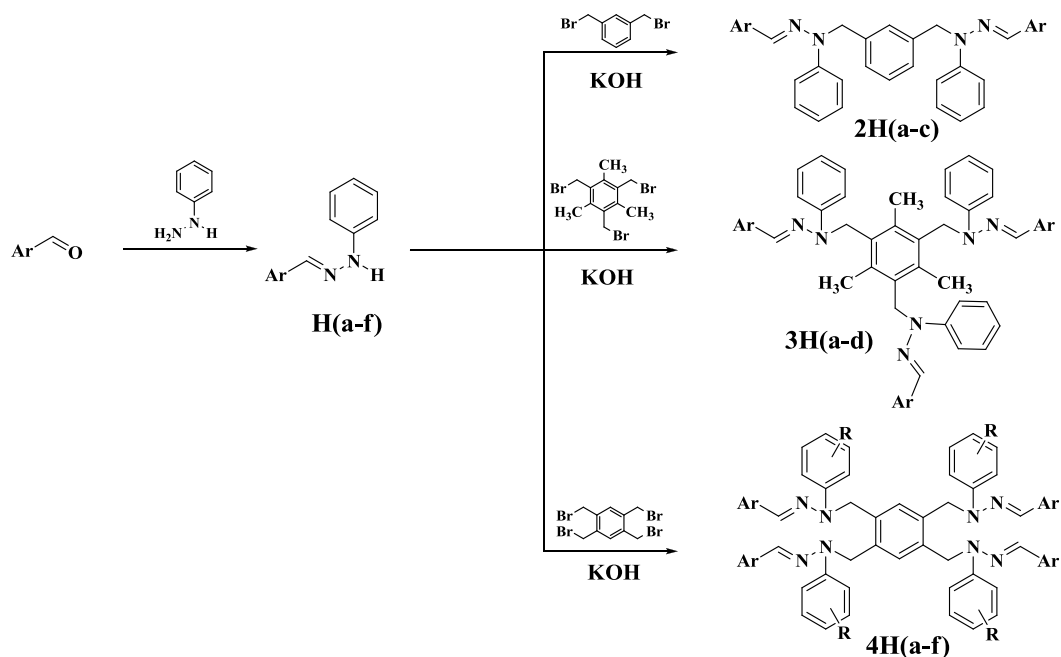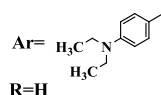

Figure 19. Structures of the linkesr used for the synthesis of the HTM's
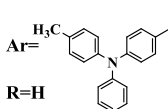
At the second "Click" stage three different compounds (**Figure 19**) with two, three and four methylbenzene branches were tested as linkers in order to get high molecular weight molecules with stable amorphous state.
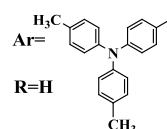
32

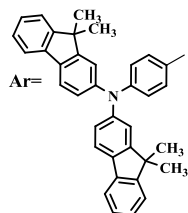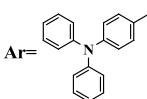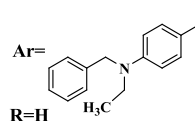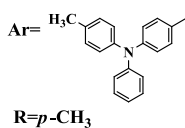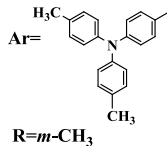**Figure 20**. Synthesis scheme of the branched hydrazones

Reaction conditions for all compounds were similar. After dissolving reagents in acetone and addition of the powdered 85% KOH mixture were stirred at reflux for one hour. Dihydrazones **2H(a,b)** and tetrahydrazones **4H(a-d)** crystallized during the reaction and were purified by non-chromatographic methods (filtration and washing). All trihydrazones **3H(a-d)**, dihydrazone **2Hc** and tetrahydrazones **4H(e,f)** did not formed crystalline state during the reaction and after column chromatography were obtained as amorphous solids. Yields were in a range of

51-79%. It is a good values for a high molecular weight branched molecules. All materials were characterized by ^{1}H NMR, ^{13}C NMR and elemental analysis.

4.1.2. Properties

In order to determine aggregation state of the synthesized HTM's DSC analysis were performed. Results are summarized in **Table 1**. During first heating cycle **2H(a-c)** and **4H(a-d, f)** showed melting process (**Figure 21** top left). For **4Ha** after first melting recrystallization were observed, followed by two additional more sharp endothermic transitions (**Figure 21** top right). It means that there exist several crystalline states with different molecules arrangement. After cooling on the second heating only glass transition were observed for all of these materials. All trihidrazones (**3H(a-d)**) and one of the tetrahydrazones (**4He**) exists only in an amorphous state (**Figure 21** bottom).
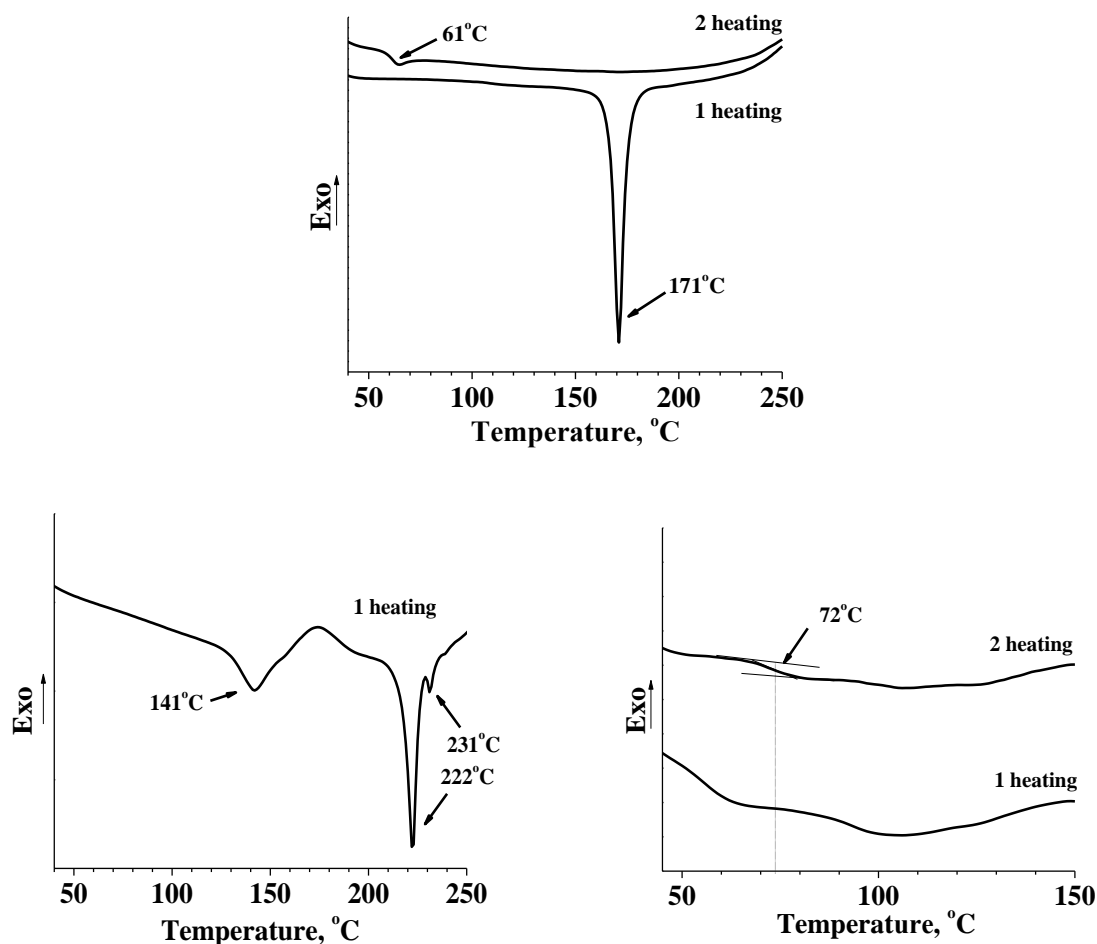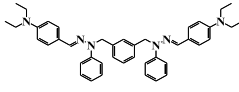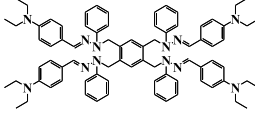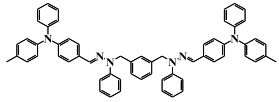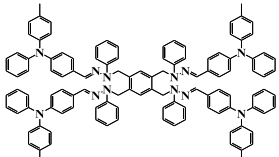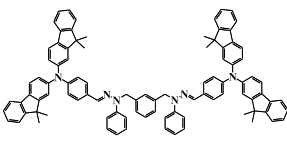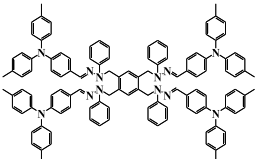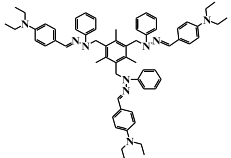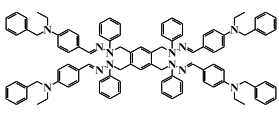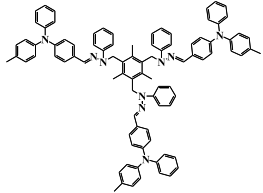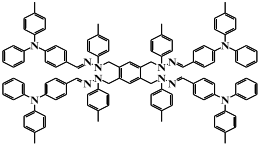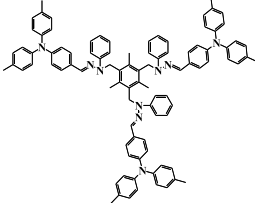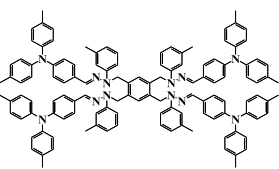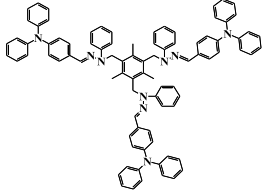

Figure 21. DSC of the **2Ha** (top left), **4Ha** (Top right) and **3Hb**(bottom)

Table 1. Thermal properties of the synthesized branched hydrazone HTM's. [I] – capillary melting points; [II] – no crystalline transition were detected; [III] – polymorphism (from DSC); [IV] – determined from the DSC analysis second heating results

Material	T_m	T_g	Material	T_m	T_g
2Ha	167[I]	61[IV]	4Ha	141[I], 222, 231[III]	75[IV]
2Hb	134-135[I]	97[IV]	4Hb	191-192[I]	104[IV]
2Hc	195[I]	137[IV]	4Hc	143-144[I]	125[IV]
3Ha	-[II]	63[IV]	4Hd	178[I]	68[IV]
3Hb	-[II]	72[IV]	4He	-[II]	60[IV]
3Hc	-[II]	103[IV]	4Hf	66[I]	117[IV]
3Hd	-[II]	104[IV]			

Although it is very difficult to predict transition temperature several observations about amorphous state stability can be made. First of all, T_g values increase by going from dihydrazone to tetrahydrazone (+14°C for **2Ha** to **4Ha** and +7°C for **2Hb** to **4Hb**) and from trihidrazone to thetrahydrazone (+12°C for **3Ha** to **4Ha**, +32°C for **3Hb** to **4Hb** and +22°C for **3Hc** to **4Hc**). Another important thing is asymmetry of the molecule. On the example of the **3H(b-d)** it can be

seen that introduction of one methyl group in the triphenylamine chromophore have stronger influence on the T_g, as asymmetry of the molecule increase. Finally for the tetrahydrazones changes made closer to the central unit led to the fully amorphous material (**4He**).

Absorption maximums of all synthesized compounds from the solution lay in the range of 340-400 nm. As there is no conjugation through the $-CH_2-$ bond hiperchromic effect is observed with the increasing number of chromophores in the molecule. For trihidrazones hipsochromic shift is also observed. It can be related to the presence of methyl groups in the central fragment (**Figure 22**).
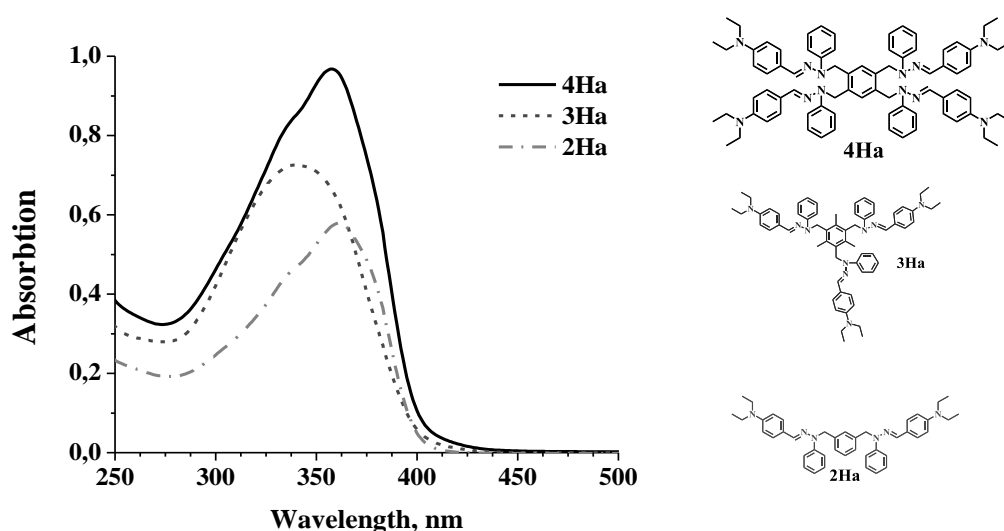
Figure 22. Absorption spectra of (**2-4)Ha**. Recorded from the 10^{-4}M solution in $CHCl_3$.

The ionization potential (I_p) was measured by electron photoemission in air[1] and are presented in the **Table 2**. Values are almost the same in a row of the compounds with same chromophore and differ for different chromophores (5-5.02 for **2Ha**, **3Ha**, **4Ha**, 5.24-5.29 for **3Hc**, **4Hc** and 5.33-5.35 for **2Hb**, **3Hb**, **4Hb**). Influence of the methyl group is in the agreement with the previously reported results for simple hydrazone molecules [61]. With the increasing number of methyl groups ionization potential is decreased. For the good performance in the perovskite solar cell I_p should be lower than the valence band of perovskite (~5.3 eV). [73]. 9 out of 13 synthesized compounds have suitable ionization potential values.

To further investigate electrical properties of the synthesized compounds hole drift mobility was measured by time of flight technique[1] (**Table 2**). Films of synthesized compounds were prepared by casting technique from a solution. Tetrahydrazones **4H(a-c)** tended to crystallize or formed inhomogeneous layer, that is why only approximate hole drift mobilities

---

[1] I_p and μ were measured at the Department of Solid State Electronics, Vilnius University by dr. V. Gaidelis and dr. V. Jankauskas.

are reported. As expected, compounds with triphenylamine based chromophores showed ca. one order of magnitude higher results than corresponding compounds with *N,N*-diethylaniline or *N*-benzyl-*N*-ethylaniline fragment. In the series of compounds with the same chromophores dihydrazones have noticeably higher mobilities. Best value was obtained for the **2Hc**. In the high electrical field it exceeds 10^{-3} cm^2/V·s. It is a very good result for the amorphous HTM.

Table 2. Ionization potentials and drift mobilities of the branched hydrazones. [1] - at an electric field 6.4×10^5V/cm.

Material	μ_0, (cm^2/V·s)	μ, (cm^2/V·s)[I]	I_p, eV
2Ha	3×10^{-7}	8×10^{-5}	5.02
2Hb	7.4×10^{-5}	1.3×10^{-3}	5.35
2Hc	4.2×10^{-5}	3×10^{-3}	5.30
3Ha	3.5×10^{-8}	2.2×10^{-5}	5.0
3Hb	4.6×10^{-6}	2.0×10^{-4}	5.33
3Hc	5×10^{-6}	6×10^{-4}	5.24
3Hd	8×10^{-7}	1.1×10^{-4}	5.4
4Ha		$\sim 1 \times 10^{-5}$	5.0
4Hb		$\sim 6.7 \times 10^{-4}$	5.35
4Hc		$\sim 5 \times 10^{-4}$	5.29
4Hd	1.2×10^{-7}	3.2×10^{-5}	5.13
4He	3×10^{-7}	1.2×10^{-4}	5.3
4Hf	$\sim 2 \times 10^{-5}$	5×10^{-4}	5.23

2Hc with the best hole drift mobility was tested in the perovskite solar cell[2]. Unfortunately, only 0.07% efficiency was reached.

4.2. Hydrazone polymers

Inspired by the relatively high yields and simple reaction conditions of the "Click" reaction polymeric hydrazones were synthesized. In this case dialdehydes were used for the synthesis of the intermediate compounds **DH(a-b)** which were further polymerized via "Click" reaction (**Figure 23**). Main advantage of this scheme is that metal complexes (such as Pd and Ni) are not

---

[2] Preliminary tests of the performance in solar cells with **2H3** and **PH2** were performed at the Photovoltaic and Optoelectronic Device Group, University of Oxford, United Kingdom by dr. James Ball.

used for the synthesis, as it is known that even traces of the catalyst in the final product dramatically decrease performance of the material. Methoxy groups were introduced in order to reduce ionization potential.
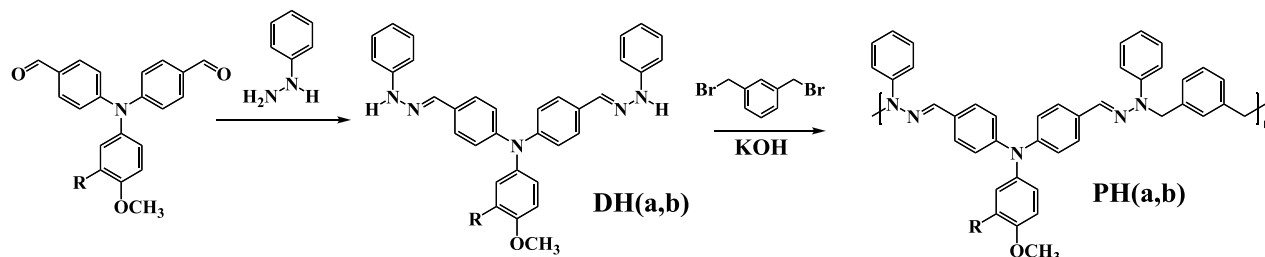
Figure 23. Synthesis scheme of the polyhydrazones **PHa** (R=H) and **PHb**(R=CH$_3$).

As intermediate **DHa** had poor solubility in acetone, solvent was changed to THF. For the polymer **PHa** optimization of the reaction time was performed. Results are shown in **Figure 24**.
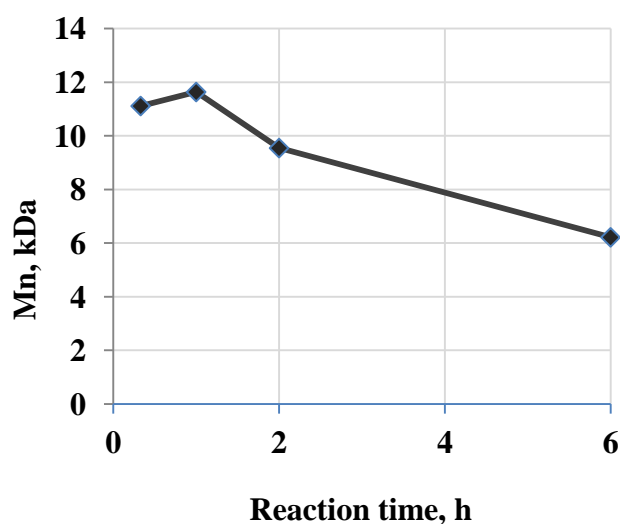
Figure 24. Number average molecular weight (Mn) dependence on the reaction time.

It can be seen that high number average molecular weight (~10 kDa) can be obtained after very short reaction times. Already after 20 min. Mn of 11 kD were achieved reaching maximum after 1 h. With the longer reaction times slow decrease in Mn is observed. This can be attributed to the thermal degradation of the hydrazone moiety under influence of the KOH, temperature, solvent and O$_2$.

DHb structure has only small difference from the **DHa**. That is why the same time (1h.) was used for the synthesis. Mn was smaller but still relatively high (~9 kDa).

I$_p$ of the synthesized compounds are almost the same (5.23 for **PHa** and 5.20 for **PHb**) and <5.3 eV. Hole drift mobility of the **PHb** at the high electrical field almost reach 10^{-3} cm^2/V·s (**Table 3**)[1] [(p. 39)].

Table 3. Properties of the **PHa** and **PHb**.[I] - at an electric field 6.4×10^5V/cm.

	PHa	PHb
Number average molecular weight **Mn**	12151	8958
Polydispersity index **Mw/Mn**	3.48	1.84
I_p, eV	5.23	5.20
μ_0, $(cm^2/V \cdot s)$	5×10^{-6}	1.5×10^{-5}
μ, $(cm^2/V \cdot s)^I$	6×10^{-4}	9×10^{-4}

As photoelectrical properties of the **DHb** are good for the non-conjugated polymers performance in perovskite solar cell was tested. In this case better results were achieved, but still only ~1.2% efficiency was achieved[2 (p. 40)].

4.2.1. Conclusion hydrazones

Proposed synthesis scheme can be used for the fast synthesis of the novel HTM's. Almost without changes it is suitable for the synthesis of a large variety of compounds. By molecular engineering stable amorphous state can be achieved. The problem is that hydrazones did not showed good or even average performance in perovskite solar cells. It can be attributed to poor energy level matching and inconsistency with oxidative additives.

4.3.   Diphenylamine substituted carbazole twin molecules

In order to adopt "Click" reaction for the synthesis of the more suitable HTM's for perovskite solar cells several changes in scheme were made. Hydrazone was changed with carbazole. Further functionalization with diphenylamine derivative is also of the most importance, as it ensures good photoelectrical properties and matching with dopants. It is the common fragment in most of the alternatives to **Spiro-OMeTAD**. As the best hole drift mobilities were achieved for dihydrazones, bis(bromomethyl)benzenes were used for the synthesis. All three possible isomers were tested.

4.3.1. Synthesis

The synthesis route to these hole transporting materials involves the "click" reaction of suitable bis(bromomethyl)benzene (dibromoxylene) with 3,6-dibromocarbazole, followed by the palladium catalyzed C–N cross-coupling reaction with diphenylamine derivatives (**Figure 25**).
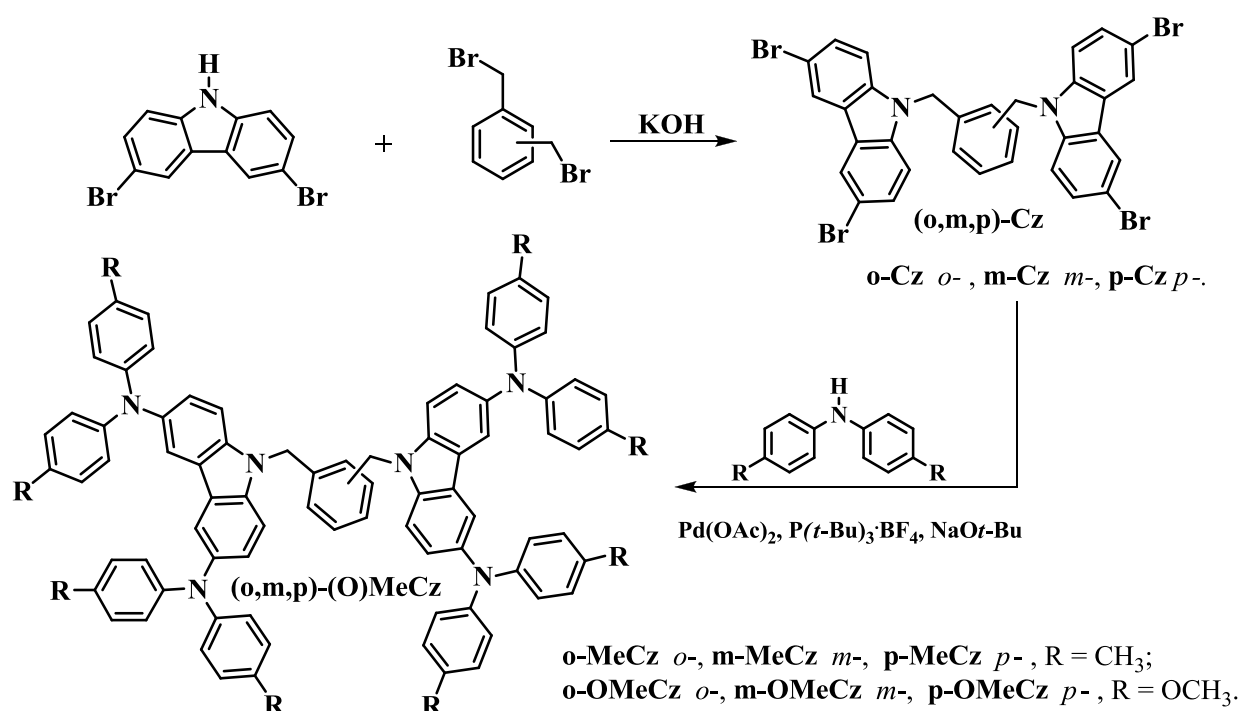
Figure 25. Synthesis of the diphenylamine substituted carbazole twin derivatives

Intermediate compounds **(o,m,p)-Cz** were formed already after 10 min. at room temperature. After filtration and washing with water these compounds were directly used for the further synthesis. Final materials **(o,m,p)-(O)MeCz** were purified by column chromatography. Overall yield (of two stages) reaches 75%.

4.3.2. Properties

DSC analysis (**Table 4**) showed that HTM's with methoxy groups does not form crystalline state. The highest T_g values are for *p-* substituted central fragment, the lowest – for *o-*. Destruction temperatures are high enough (lowest for **o-OMeCz** 389°C). In comparison to the **Spiro-OMeTAD** our proposed compounds have an advantage. **Spiro-OMeTAD** can form crystalline state and glass transition temperature is 34-48°C lower than of the twin molecules **(o,m,p)-OMeCz**. Crystallization of the HTM is undesired process, as under working conditions it can reduce long-term stability of the device [74].
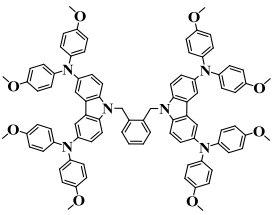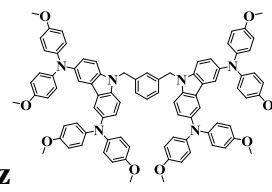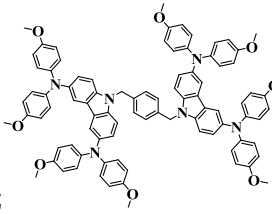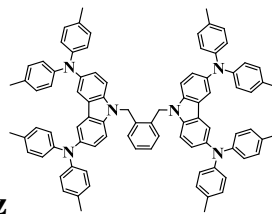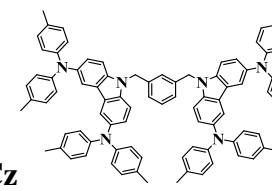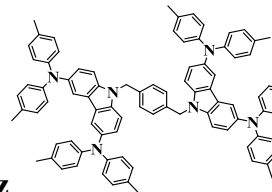
Table 4. Thermal properties of the twin molecules

Compound	T_g, °C	T_m, °C	T_d, °C
o-OMeCz	141	-	389
m-OMeCz	139	-	*391*
p-OMeCz	144	-	391
o-MeCz	158	233	399
m-MeCz	151	-	402
p-MeCz	163	337	399
Spiro-OMeTAD	105	255	440
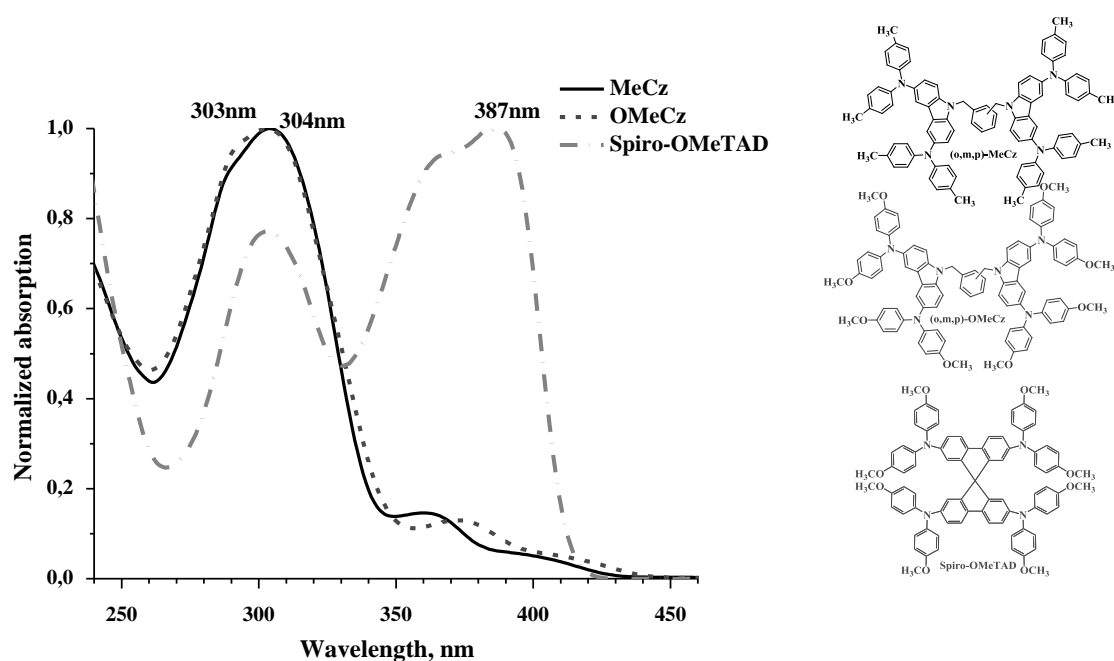
Figure 26. Optical spectra of the **(o,m,p)-(O)MeCz** Recorded from the 10^{-4}M solution in THF

UV/Vis absorption spectra of the **(o,m,p)-(O)MeCz** are shown in **Figure 26**. Major absorption occurs in the UV range. For the isomers, as can be expected, absorption is identical. Also methyl group change by methoxy introduces only small changes in optical properties. In a comparison to the **Spiro-OMeTAD** our HTM's have much lower absorption between 350-420 nm. In some cases this can be an advantage (e.g. tandem cells or cells with inverted architecture [75]).

Table 5 Ionization potential and charge mobility values of the twin molecules. [I] - at an electric field 6.4×10^5 V/cm.

Formula	Ip, eV	μ_0, (cm^2/V·s)	μ, (cm^2/V·s)[I]
o-OMeCz	5.04	2×10^{-5}	6×10^{-4}
m-OMeCz	5.06	1×10^{-4}	4.6×10^{-3}
p-OMeCz	5.07	8×10^{-6}	4×10^{-5}
o-MeCz	5.20	3.5×10^{-5}	7.8×10^{-4}
m-MeCz	5.25	8×10^{-6}	3.7×10^{-4}
p-MeCz	5.20	1.3×10^{-5}	4×10^{-4}
Spiro-OMeTAD	5.00	4×10^{-5}	5×10^{-4}

Functional groups attached at the ends of the molecules have noticeable influence on ionization potential. HTM's with methoxy groups have lower I_p compared with methyl containing ones (**Table 5**). Interesting tendency is observed in the hole drift mobilities[1 (p. 39)]. For the compounds **(o,m,p)-MeCz** with methyl group values are of the same order of magnitude.

Completely different situation is for the **(o,m,p)-OMeCz**. The highest result is of the *metha* isomer (4.6×10^{-3} cm^2/V·s at the strong fields), while for the *para* isomer it is only 4×10^{-5} cm^2/V·s. This can be attributed to the hydrogen bond formation between different molecules. It means that in some cases shape of the molecule and way of packing in the film has major influence on the hole mobility results, in some not.

4.3.3. Optical properties of the oxidized o-OMeCz
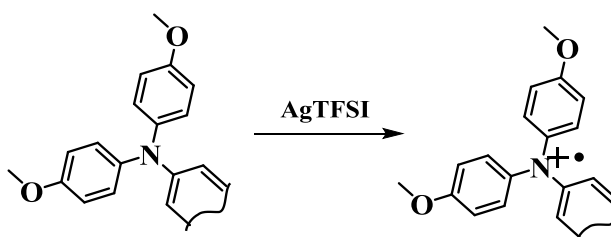
Figure 27. Oxidation of the methoxydiphenylamine fragment

As in a device HTM is partly (20-30%) oxidized it is interesting to check properties in the oxidized state. In a similar manner to the procedure reported by prof. M. McGehee [41] oxidation of the **o-OMeCz** with **AgTFSI** were performed (**Figure 27**) and optical properties investigated by the UV/Vis/NIR spectroscopy.
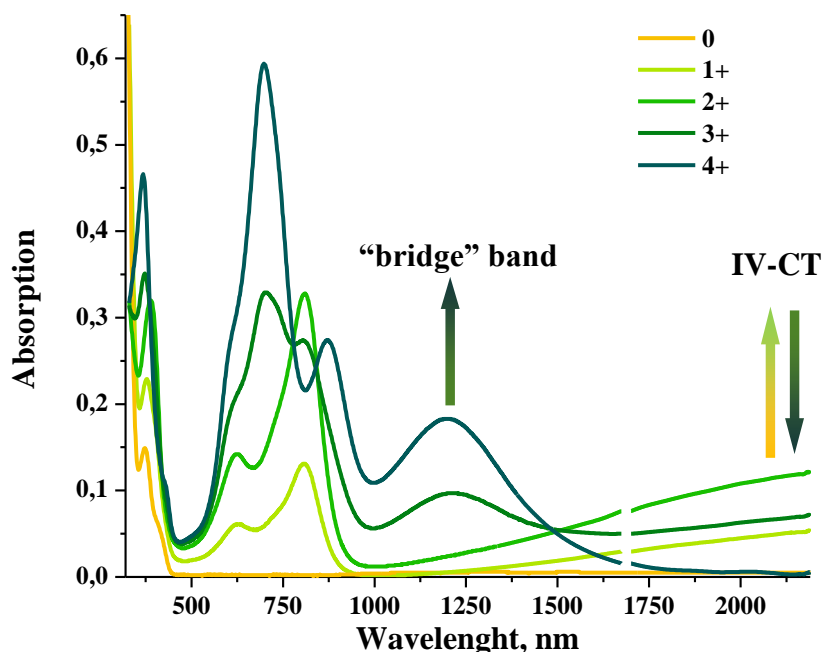
Figure 28. Absorption spectra of the different **o-OMeCz** oxidation states

Upon addition of the oxidant diphenylamine moieties are transforming into cation radicals and novel strong absorption bands appear in the visible and near-infrared ranges. As there are 4 diphenylamine fragments in the molecule up to 4+ oxidation state molecule can be obtained. In

43

the spectra there can be seen appearance of the very broad band in the NIR region with the maximum >2200 nm by going from 0 to 2+ oxidation state and consequent decrease of it from 2+ to 4+. This band can be attributed to the intervalence charge transfer (IV-CT). The band at 1200 nm is most probable due to the electron transfer from carbazole unit to diphenylamine and appears only from the 2+ [76].Such behavior indicates that oxidation occurs stepwise on the two fragments independently (**Figure 29**).
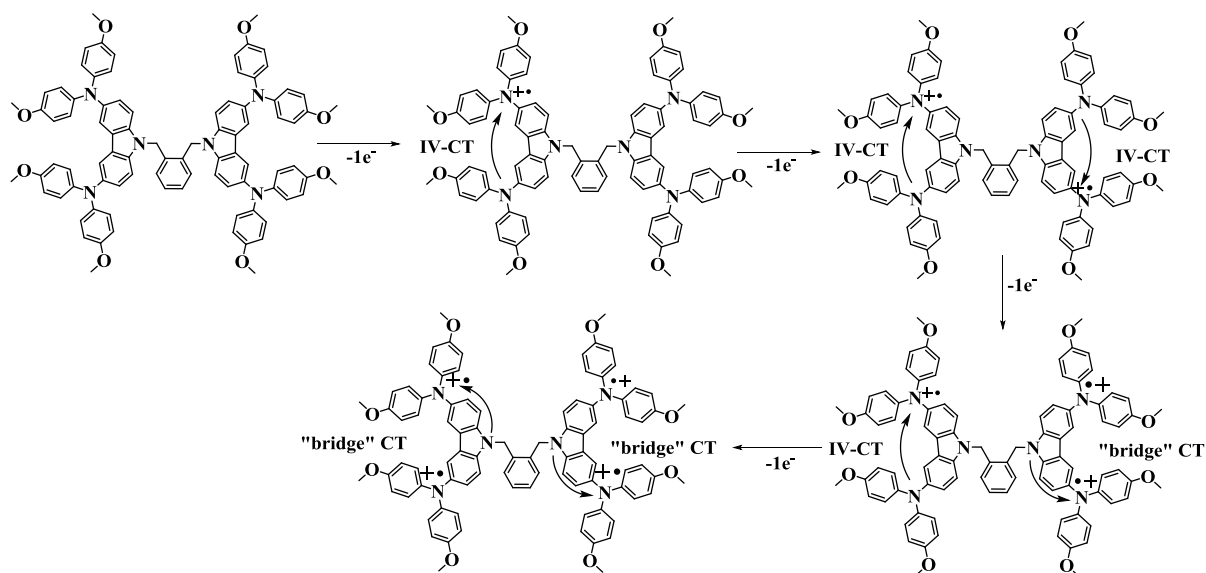
Figure 29. Oxidation process and absorption band formation

State of the highest oxidation (4+) is quite unstable. Already after several hours at room temperature significant changes in absorption are observed (**Figure 30**). On the other hand 2+ oxidized molecules did not showed signs of decomposition.
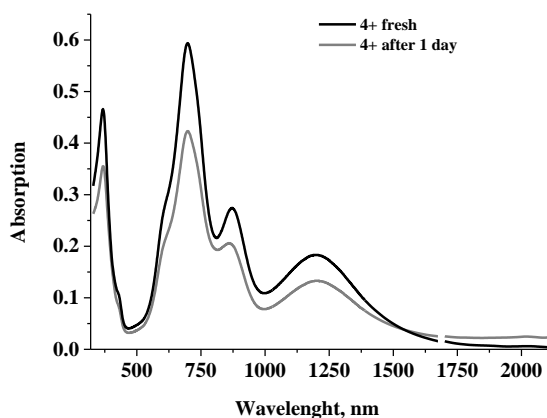
Figure 30. Degradation of the **o-OMeCz^{4+}(TFSI$^-$)$_4$**.

Performance in perovskite solar cells were investigated at the *École Polytechnique Fédérale de Lausanne*[3]. Compounds with the methyl group did not shove any reasonable performance. With **m-OMeCz** 6.7% efficiency was achieved. The most exciting result was achieved with the perovskite solar cell employing **o-OMeCz** as a HTM. Highest reached efficiency is 16.91%. For the best of our knowledge it is one of the best reported values for the small molecule hole transporting materials. Device of the same construction but with **Spiro-OMeTAD** showed 18.36% efficiency.

---

[3] Perovskite solar cells with **(o,m,p)-(O)MeCz** were constructed and tested at the Laboratory for Photonics and Interfaces, École Polytechnique Fédérale de Lausanne, Switzerland by Paul Gratia.

CONCLUTIONS

1. In the work novel hole transporting materials were synthesized by the "Click" reaction in a fast and efficient way. Perovskite solar cells with 1,2-bis[3,6-(4,4-dimethoxydiphenylamino)-9*H*-carbazol-9-methyl]benzene (**o-OMeCz**) shows up to 16.91% efficiency. It is one of the best results for the small molecule hole transporting materials.

2. Branched hydrazone HTM's by "click" chemistry reaction with three different linkers (1,3-bis(bromomethyl)benzene, 2,4,6-tris(bromomethyl)mesitylene and 1,2,4,5-tetrakis(bromomethyl)benzene) were synthesized and investigated. It was shown that:

   - While optical properties and I_p are mostly determined by the chromophore, aggregation state and hole drift mobilities are strongly dependent on the linker.
   - Best hole drift mobilities are of the dihydrazones with the best result for 1,3-bis{1-phenyl-2-[4-(bis(9,9-dimethyl-9*H*-fluoren-2-yl)amino)benzyliden]hydrazinmethyl}benzene (**2Hc**) reaching 3×10^{-3} cm^2/V·s mobility at an electric field 6.4×10^5V/cm.

3. In the similar manner two hydrazone polymers were synthesized and properties investigated. It was shown that:

   - Optimal reaction time for the synthesis of *poly*{4,4'-[(4-methoxyphenyl)azanediyl]dibenzaldehyde bis(*N*-phenylhydrazone)-*alt*-1,3-bis(bromomethyl)benzene} (**PHa**) is 1h.
   - Perovskite solar cell with *poly*{ 4,4'-[(4-methoxy-3-methylphenyl)azanediyl]dibenzaldehyde bis(*N*-phenylhydrazone)-*alt*-1,3-bis(bromomethyl)benzene} (**PHb**) efficiency is 1.2%.

4. "Click" chemistry scheme was adopted for the diphenylamine substituted carbazole twin molecules synthesis and 6 compounds were synthesized. It was shown that:

   - Stable amorphous state materials can be obtained.
   - Way of molecules packing in a film can have major influence on the hole drift mobility.
   - Upon oxidation absorption in visible and near-infrared increases dramatically.

REFERENCES

[1]   Maehlum M.A. What is the Potential of Solar Energy? 2013 [viewed 30 05 2015]. Available from: http://energyinformative.org/potential-of-solar-energy/].

[2]   Kearns D., Calvin M. Photovoltaic Effect and Photoconductivity in Laminated Organic Systems. *The Journal of Chemical Physics*, 1958, vol. 29, p. 950

[3]   Ghosh A.K., Morel D.L., Feng T., Shaw R.F., Rowe C.A. Photovoltaic and rectification properties of Al/Mg phthalocyanine/Ag Schottky-barrier cells. *Journal of Applied Chemistry*, 1974, vol. 45, p. 230

[4]   Tang C.W., Albrecht A.C. Photovoltaic effects of metal–chlorophyll-a–metal sandwich cells. *The Journal of Chemical Physics*, 1975, vol. 62, p. 2139

[5]   Ghosh A.K., Feng T. Merocyanine organic solar cells. *Journal of Applied Physics*, 1978, vol. 49, p. 5982

[6]   Tang C.W. Two-layer organic photovoltaic cell. *Applied Physics Letters*, 1986, vol. 48, p. 183

[7]   Yu G.,Gao J., Hummelen J.C., Wudl F., Heeger A.J. Polymer Photovoltaic Cells: Enhanced Efficiencies via a Network of Internal Donor-Acceptor Heterojunctions. *Science*, 1995, vol. 270, p. 1789-1791

[8]   O'Regan B., Grätzel M. A low-cost, high-efficiency solar cell based on dye-sensitized colloidal TiO2 films. *Nature*, 1991, vol. 353, p. 737-740

[9]   National Center for Photovoltaics. Research cell efficiency records. 2015 [viewed 30 05 2015]. Available from: http://www.nrel.gov/ncpv/images/efficiency_chart.jpg

[10]   Bach U., Lupo D., Comte P., Moser J.E., Weissörtel F., Salbeck J., Spreitzer H., Grätzel M. Solid-state dye-sensitized mesoporous TiO2 solar cells with high photon-to-electron conversion efficiencies. *Nature*, 1998, vol. 395, p. 583-585

[11]   Mozer A.J., Panda D.K., Gambhir S., Winther-Jensen B., Wallace G.G. Microsecond Dye Regeneration Kinetics in Efficient Solid State Dye-Sensitized Solar Cells Using a Photoelectrochemically Deposited PEDOT Hole Conductor. *Journal of the American Chemical Society*, 2010, vol. 132 (28), p. 9543-9545.

[12]   Roh D.K., Chi W.S., Jeon H., Kim S.J., Kim J.H. High Efficiency Solid-State Dye-Sensitized Solar Cells Assembled with Hierarchical Anatase Pine Tree-like TiO$_2$ Nanotubes. *Advanced Functional Materials*, 2013, vol. 24, p. 379-386

[13] Perovskites may give silicon solar cells a run for their money. 2015 [viewed 30 05 2015]. Available from: http://www.economist.com/news/science-and-technology/21651166-perovskites-may-give-silicon-solar-cells-run-their-money-crystal-clear

[14] Wenk H.R., Bulakh A. Minerals: Their Constitution and Origin. Cambridge University Press, 2004

[15] Snaith H. J. Perovskites: The Emergence of a New Era for Low-Cost, High-Efficiency Solar Cells. *J. Phys. Chem. Lett.* 2013, vol. *4* (21),p. 3623–3630.

[16] Kojima A., Teshima K., Shirai Y., Miyasaka T. Novel Photoelectrochemical Cell with Mesoscopic Electrodes Sensitized by Lead-Halide Compounds. 210th ECS Meeting, Cancun, Mexico, Oct. 29–Nov. 3, 2006.

[17] Kojima A., Teshima K., Shirai Y., Miyasaka T. Organometal Halide Perovskites as Visible-Light Sensitizers for Photovoltaic Cells. *Journal of the American Chemical Society*, 2009, vol. 131, p. 6050–6051

[18] Im J.H., Lee C.R., Lee J.W., Park S.W., Park N.G. 6.5% Efficient Perovskite Quantum-Dot-Sensitized Solar Cell. *Nanoscale* 2011, *3* (10), 4088–4093.

[19] Lee M. M., Teuscher J., Miyasaka T., Murakami T. N., Snaith H. J. Efficient Hybrid Solar Cells Based on Meso-Superstructured Organometal Halide Perovskites. *Science* 2012, vol. 338 (6107), p. 643–647.

[20] Kim H.-S., Lee C.-R., Im J.H., Lee K.B., Moehl T., Marchioro A., Moon S.J., Humphry-Baker R., Yum J.H., Moser J.E., et al. Lead Iodide Perovskite Sensitized All-Solid-State Submicron Thin Film Mesoscopic Solar Cell with Efficiency Exceeding 9%. *Scientific Reports,* 2012, vol. 2, p. 591.

[21] Shi J., Dong J., Lv S., Xu Y., Zhu L., Xiao J, Xu X, Wu H., Li D., Luo Y., Meng Q. Hole-conductor-free perovskite organic lead iodide heterojunction thin-film solar cells: High efficiency and junction property. *Applied Physics Letters*, 2014, vol. 104, p. 63901

[22] Oxford PV. Next generation solar power. 2015. [viewed 30 05 2015]. Available from: http://www.oxfordpv.com/sites/www.oxfordpv.com/files/media-downloads/general/oxford-pv-introduction-152.pdf

[23] Bi C., Shao Y., Yuan Y., Xiao Z., Wang C., Gaob Y., Huang J. Understanding the formation and evolution of interdiffusion grown organolead halide perovskite thin films by thermal annealing. *Journal of Materials Chemistry A,* 2014, vol. 2, p. 18508-18514

[24]   Docampo P., Hanusch F.C., Stranks S.D., Döblinger M., Feckl J.M., Ehrensperger M., Minar N.K., Johnston M.B., Snaith H.J., Bein T. Solution Deposition-Conversion for Planar Heterojunction Mixed Halide Perovskite Solar Cells. *Advanced Energy Materials*, 2014, vol. 14, p. 1400355

[25]   Chen Q., Zhou H., Hong Z., Luo S., Duan H.S., Wang H.H., Liu Y., Li G., Yang Y. Planar Heterojunction Perovskite Solar Cells via Vapor-Assisted Solution Process. *Journal of the American Chemical Society*, 2013, vol. 136(2), p. 622-625.

[26]   Liu M., Johnston M.B., Snaith H.J. Efficient planar heterojunction perovskite solar cells by vapour deposition. *Nature*, 2013, vol. 501, p. 395–398

[27]   Longo G., Gil-Escrig L., Degen M.J., Sessolo M., Bolink H.J. Perovskite solar cells prepared by flash evaporation. *Chemical Communications*, 2015, vol. 51, p. 7376-7378

[28]   Ball J.M., Lee M.M., Hey A., Snaith H.J. Low-temperature processed meso-superstructured to thin-film perovskite solar cells. *Energy & Environmental Science*, 2013, vol. 6, p. 1739-1743.

[29]   Habisreutinger S.N., Leijtens T., Eperon G.J., Stranks S.D., Nicholas R.J., Snaith H.J. Carbon Nanotube/Polymer Composites as a Highly Stable Hole Collection Layer in Perovskite Solar Cells. *Nano Letters*, 2014, vol. 14, p. 5561-5568

[30]   Noel N.K., Stranks S.D., Abate A., Wehrenfennig C., Guarnera S., Haghighirad A.A., Sadhanala A., Eperon G.E., Pathak S.K., Johnston M.B., Petrozza A., Herza L.M., Snaith H.J. Lead-free organic–inorganic tin halide perovskites for photovoltaic applications. *Energy & Environmental Science*, 2014, vol. 7, p. 3061-3068

[31]   Spiro-OMeTAD price at Sigmaaldrich (331.00 EUR for 1 g) [viewed 30 05 2015]. Available from: http://www.sigmaaldrich.com/catalog/product/aldrich/792071,

Spiro-OMeTAD price at Solaronix (619.00 CHF for 1 g) [viewed 30 05 2015]. Available from: http://shop.solaronix.com/spiro-ometad.html

[32]   Salbeck J., Yu N., Bauer J., Weissörtel F., Bestgen H. Low Molecular Organic Glasses for Blue Electroluminescence. *Synthetic Metals,* 1997, vol. 91 (1-3), p. 209–215.

[33]   Bach U., Lupo D., Comte P., Moser J.E., Weissortel F., Salbeck J., Spreitzer H., Gratzel M. Solid-State Dye-Sensitized Mesoporous TiO2 Solar Cells with High Photon-to-Electron Conversion Efficiencies. *Nature,* 1998, vol. *395* (6702), p. 583–585.

[34]   Bach U. Solid-state dye-sensitized mesoporous TiO_2 solar cells. PhD thesis, EPFL, Switzerland, 2000

[35] Saragi T.P.I., Spehr T., Siebert A., Fuhrmann-Lieker T., Salbeck J. Spiro Compounds for Organic Optoelectronic. *Chemical Reviews,* 2007, vol. 107 (4), p. 1011–1065.

[36] Clarkson R.G., Gomberg M. Spirans with four aromatic radicals on the spiro atom. *Journal of the American Chemical Society,* 1930, vol. 52 (7), p. 2881–2891.

[37] WU X.M., CHEN X.C., CAO X.P., PAN X.F. A practical method to synthesize 2,2',7,7'-tetraiodo-9,9'-spirobifluorene. *Ganguang Kexue Yu Guang Huaxue*, 2001, vol. 19, p. 161

[38] Poriel C., Ferrand Y., Juillard S., Le Maux P., Simonneaux G. Synthesis and Stereochemical Studies of Di and Tetra 9,9′-Spirobifluorene Porphyrins: New Building Blocks for Catalytic Material. *Tetrahedron,* 2004, vol. 60 (1), p. 145–158.

[39] Weissörtel. F. Synthese und Characterisierung spiroverknüpfter niedermolecularer Gläser für optoelektronische Anwendungen. Ph.D. Thesis, University of Regensburg, Germany, 1999.

[40] Hartwig J.F. Übergangsmetall-Katalysierte Synthese von Arylaminen Und Arylethern Aus Arylhalogeniden Und -Triflaten: Anwendungen Und Reaktionsmechanismus. *Angewandte Chemie,* 1998, vol. 110 (15), p. 2154–2177.

[41] Nguyen W.H., Bailie C.D., Unger E.L., McGehee M.D. Enhancing the Hole-Conductivity of Spiro-OMeTAD without Oxygen or Lithium Salts by Using spiro(TFSI)$_2$ in Perovskite and Dye-Sensitized Solar Cells. *Journal of the American Chemical Society,* 2014, vol. 136 (31), p. 10996–11001.

[42] Abate A., Leijtens T., Pathak S., Teuscher J., Avolio R., Errico M.E., Kirkpatrik J., Ball J.M., Docampo P., McPherson I., et al. Lithium Salts as "Redox Active" P-Type Dopants for Organic Semiconductors and Their Impact in Solid-State Dye-Sensitized Solar Cells. *Physical Chemistry Chemical Physics,* 2013, vol. 15 (7), p. 2572–2579.

[43] Xu B., Huang J., Ågren H., Kloo L., Hagfeldt A., Sun L. AgTFSI as P-Type Dopant for Efficient and Stable Solid-State Dye-Sensitized and Perovskite Solar Cells. *ChemSusChem,* 2014, vol. 7 (12), p. 3252–3256.

[44] Burschka J., Dualeh A., Kessler F., Baranoff E., Cevey-Ha N.L., Yi C., Nazeeruddin M.K., Grätzel M. Tris(2-(1H-Pyrazol-1-yl)pyridine)cobalt(III) as P-Type Dopant for Organic Semiconductors and Its Application in Highly Efficient Solid-State Dye-Sensitized Solar Cells. *Journal of the American Chemical Society,* 2011, vol. 133 (45), p. 18042–18045.

[45]   Nazeeruddin M.K., Kay A., Rodicio I., Humphry-Baker R., Muller E., Liska P., Vlachopoulos N., Gratzel M. Conversion of light to electricity by cis-X2bis(2,2'-bipyridyl-4,4'-dicarboxylate)ruthenium(II) charge-transfer sensitizers (X = Cl-, Br-, I-, CN-, and SCN-) on nanocrystalline titanium dioxide electrodes. *Journal of the American Chemical Society.* 1993, vol. 115 (4), p. 6382–6390.

[46]   Noel N.K., Abate A., Stranks S.D., Parrott E., Burlakov V., Goriely A., Snaith H.J. Enhanced Photoluminescence and Solar Cell Performance via Lewis Base Passivation of Organic-Inorganic Lead Halide Perovskites. *ACS Nano,* 2014, vol. 8 (10), p. 140829182541001.

[47]   Jeon N.J., Lee H.G., Kim Y.C., Seo J., Noh J.H., Lee J., Seok S.Il. *o*-Methoxy Substituents in Spiro-OMeTAD for Efficient Inorganic-Organic Hybrid Perovskite Solar Cells. *Journal of the American Chemical Society,* 2014, vol. 136 (22), p. 7837–7840.

[48]   Jeon N.J., Lee J., Noh J.H., Nazeeruddin M.K., Grätzel M., Seok S.Il. Efficient Inorganic-Organic Hybrid Perovskite Solar Cells Based on Pyrene Arylamine Derivatives as Hole-Transporting Materials. *Journal of the American Chemical Society,* 2013, vol. 135 (51), p. 19087–19090.

[49]   Li H., Fu K., Hagfeldt A., Grätzel M., Mhaisalkar S.G., Grimsdale A.C. A Simple 3,4-Ethylenedioxythiophene Based Hole-Transporting Material for Perovskite Solar Cells. *Angewandte Chemie International Edition in English,* 2014, vol. 53 (16), p. 4085–4088.

[50]   Li H., Fu K., Boix P.P., Wong L.H., Hagfeldt A., Grätzel M., Mhaisalkar S.G., Grimsdale A.C. Hole-Transporting Small Molecules Based on Thiophene Cores for High Efficiency Perovskite Solar Cells. *ChemSusChem,* 2014, vol. 7 (12), p. 3420–3425.

[51]   Xu B., Sheibani E., Liu P., Zhang J., Tian H., Vlachopoulos N., Boschloo G., Kloo L., Hagfeldt A., Sun L. Carbazole-Based Hole-Transport Materials for Efficient Solid-State Dye-Sensitized Solar Cells and Perovskite Solar Cells. *Advanced Materials,* 2014, vol. 26 (38), p. 6629–6634.

[52]   Sung S. Do Kang M.S., Choi I.T., Kim H.M., Kim H., Hong M., Kim H.K., Lee W. I. 14.8% Perovskite Solar Cells Employing Carbazole Derivatives as Hole Transporting Materials. *Chemical Communications,* 2014, vol. 50 (91), p. 14161–14163.

[53]   Conings B., Baeten L., De Dobbelaere C., D'Haen J., Manca J., Boyen H.G. Perovskite-Based Hybrid Solar Cells Exceeding 10% Efficiency with High Reproducibility Using a Thin Film Sandwich Approach. *Advanced Materials,* 2014, vol. 26 (13), p. 2041–2046.

[54]   Guo Y., Liu C., Inoue K., Harano K., Tanaka H., Nakamura E. Enhancement in the Efficiency of an Organic–inorganic Hybrid Solar Cell with a Doped P3HT Hole-Transporting Layer on a Void-Free Perovskite Active Layer. *Journal of Materials Chemistry A,* 2014, vol. 2 (34), p. 13827–13830.

[55]   Heo J.H., Im S.H., Noh J.H., Mandal T.N., Lim C.S., Chang J.A., Lee Y.H., Kim H., Sarkar A., Nazeeruddin M.K., et al. Efficient Inorganic–organic Hybrid Heterojunction Solar Cells Containing Perovskite Compound and Polymeric Hole Conductors. *Nature Photonics* 2013, vol. 7 (6), p. 486–491.

[56]   Jeon N.J., Noh J.H., Yang W.S., Kim Y.C., Ryu S., Seo J., Seok S.Il. Compositional Engineering of Perovskite Materials for High-Performance Solar Cells. *Nature* 2015, vol. 517 (7535), p. 476–480.

[57]   Liu J., Wu Y., Qin C., Yang X., Yasuda T., Islam A., Zhang K., Peng W., Chen W., Han L.A. Dopant-Free Hole-Transporting Material for Efficient and Stable Perovskite Solar Cells. *Energy & Environmental Science,* 2014, vol. 7 (9), p. 2963.

[58]   Kolb H.C., Finn M.G., Sharpless K.B. Click Chemistry: Diverse Chemical Function from a Few Good Reactions. *Angewandte Chemie International Edition*, 2001, vol. 40 (11), p. 2004–2021.

[59]   Kolb H.C., Sharpless K.B. The Growing Impact of Click Chemistry on Drug Discovery. *Drug Discovery Today,* 2003, vol. 8 (24), p. 1128–1137.

[60]   Magomedov A. Krūvininkus transportuojančių molekulinių stiklų su hidrazono fragmentu efektyvus sintezės. BSc thesis, KTU, Lithuania, 2013

[61]   Urnikaite S., Daskeviciene M., Malinauskas T., Jankauskas V., Getautis V. Study on the influence of methyl groups and their location on properties of triphenylamino-based charge transporting hydrazones. *Monatshefte fur Chemie*, 2009, vol. 140(12), p. 1453-1458

[62]   Harwood L.M., Moody C.J. Organic Chemistry, Principles and Practice. O. Mead et al. Eds., Blackwell science, 1989

[63]   Miyamoto E., Yamaguchi Y., Yokoyama M. Ionization potential of organic pigment film by atmospheric photoelectron emission analysis. *Electrophotography*, 1989, vol. 28, p. 364-370.

[64]   Montrimas E., Gaidelis V., Pazera A. The discharge kinetics of negatively charged Se electrophotographic layers. *Lithuanian Journal of Physics,* 1966, vol. 6, p. 569-578

[65]   Qin P., Paek S., Dar M.I., Pellet N., Ko J., Grätzel M., Nazeeruddin M. K. Perovskite Solar Cells with 12.8% Efficiency by Using Conjugated Quinolizino Acridine Based Hole Transporting Material. *Journal of the American Chemical Society,* 2014, vol. 136, p. 8516-8519.

[66]   Vicini P., Incerti M., La Colla P., Loddo R. Anti-HIV Evaluation of Benzo[d]isothiazole Hydrazones. *European Journal of Medicinal Chemistry,* 2009, vol. 44 (4), p. 1801–1807.

[67]   Kobayashi S., Mori Y., Fossey J.S., Salter M.M. Catalytic Enantioselective Formation of C-C Bonds by Addition to Imines and Hydrazones: A Ten-Year Update. *Chemical Reviews,* 2011, vol. 111 (4), p. 2626–2704.

[68]   Su X., Aprahamian I. Hydrazone-Based Switches, Metallo-Assemblies and Sensors. *Chemical Society Reviews,* 2014, vol. 43 (6), p. 1963–1981.

[69]   Lygaitis R., Getautis V., Grazulevicius J. V. Hole-Transporting Hydrazones. *Chemical Society Reviews*, 2008, vol. 37 (4), p. 770–788.

[70]   Jubran N., Tokarski Z., Getautis V., Grazulevicius J., Paulauskaite I., Lozano J.R., Gaidelis V., Jankauskas V. Poly(hydrazone)-based charge transport materials. US 20050221212 A1 06 10 2005

[71]   Nam H., Kang D.H., Kim J.K., Park S.Y. Synthesis of Hole-Transporting Hydrazone Dendrimers. *Chemistry Letters,* 2000, vol. 11, p. 1298–1299.

[72]   Getautis V., Daskeviciene M., Malinauskas T., Jankauskas V., Sidaravicius J. Influence of the Hydroxyl Groups on the Properties of Hydrazone Based Molecular Glasses. *Thin Solid Films,* 2008, vol. 516 (24), p. 8979–8983.

[73]   Abrusci, A., Stranks, S. D., Docampo P., Yip H.L., Jen A.K.Y., Snaith H.J. High-Performance Perovskite-Polymer Hybrid Solar Cells via Electronic Coupling with Fullerene Monolayers. *Nano Letters,* 2013, vol. 13 (7), p. 3124–3128.

[74]   Malinauskas T., Tomkutė-Lukšienė D., Sens R., Daskeviciene M., Send R., Wonneberger H., Jankauskas V., Bruder I., Getautis V. Enhancing Thermal Stability and Lifetime of Solid-State Dye-Sensitized Solar Cells via Molecular Engineering of the Hole Transporting Material Spiro-OMeTAD. *ACS Applied Materials & Interfaces,* Article ASAP.

[75]   Malinkiewicz O., Yella A., Lee Y.H., Espallargas G.M., Graetzel M., Nazeeruddin M.K., Bolink H.J. Perovskite Solar Cells Employing Organic Charge-Transport Layers. *Nature Photonics,* 2013, vol. 8 (2), p. 128–132.

[76]   Heckmann A., Lambert C. Organic Mixed-Valence Compounds: A Playground for Electrons and Holes. *Angewandte Chemie International Edition*, 2012, vol. 51, p. 326-392

LIST OF PUBLICATIONS

Publications on the work theme

1. Gratia P., **Magomedov A.,** Malinauskas T., Daskeviciene M., Abate A., Ahmad S., Grätzel M., Getautis V., Nazeeruddin M.K. Methoxydiphenylamine substituted carbazole twin derivative: inexpensive but efficient hole transporting material for perovskite solar cells. *Angewandte Chemie* [Submitted at 23 05 2015]

2. Gratia P., Nazeeruddin M.K., Grätzel M., Getautis V., **Magomedov A.,** Malinauskas T., Daskeviciene M. Small molecule hole transporting material for optoelectronic and photoelectrochemical devices. European patent application No. 15157217.9. [Filling date 02 03 2015]

3. **Magomedov A**., Malinauskas T., Daškevičiene M., Getautis V. Simple, inexpensive and efficient hole transporting materials for perovskite solar cells. *Chemija ir cheminė technologija : studentų mokslinės konferencijos pranešimų medžiaga,* Klaipėdos universiteto leidykla, Klaipėda, 2015, p. 87-89.

4. **Magomedov A**., Jankauskas V., Getautis V. Novel hydrazone-based photoconductive polymers. *Book of abstracts of the 16-th international conference-school Advanced materials and technologies* Technologija, Kaunas, 2014, p. 159.

5. **Magomedov A**., Urnikaitė S., Getautis V. Photoconductive materials possessing two, three or four hydrazone-based chromophores. *Book of abstracts of the 15-th international conference-school Advanced materials and technologies* Technologija, Kaunas, 2013, p. 123.

6. **Magomedov A**., Urnikaitė S., Getautis V. Mono-, di-, tri-, bei tetrahidrazonų, pasižyminčių teigiamų krūvininkų pernašą, sintezė ir savybės. *Studentų mokslinės konferencijos CHEMIJA IR CHEMINĖ TECHNOLOGIJA pranešimų medžiaga.* Technologija, Kaunas, 2011, p.121-123.,

7. **Magomedov A**., Urnikaitė S., Getautis V. Molekulinių stiklų, turinčių keturis fotolaidžius hidrazono fragmentus, sintezė ir savybės. *Studentų moksliniai darbai 2010-2011 m. II dalis: konferencijos medžiaga.* UAB „Baltijos kopija", Vilnius, 2011, p. 119-120.,

8. **Magomedov A**., Urnikaitė S., Getautis V. Mono-, di- bei trihidrazonų, pasižyminčių teigiamų krūvinikų pernašą, sintezė ir savybės. *Studentų moksliniai darbai 2008-2010 m.: konferencijos pranešimų medžiaga.* Petro ofsetas, Vilnius, 2010, p. 146-147.,

Other publications

1. Gamiz-Hernandez A.P.. **Magomedov A.**, Hummer G., Kaila V.R.I. Linear Energy Relationships in Ground State Proton Transfer and Excited State Proton-Coupled Electron Transfer. *The Journal of Physical Chemistry B*, 2014, vol. 119 (6), p 2611–2619.

2. **Magomedov A.**, Urnikaitė S., Getautis V. Saulės elementui skirtas kandikinis dažiklis. *Studentų moksliniai tyrimai 2012/2013 konferencijos pranešimų santraukos, II dalis.* AB „Titnagas", Vilnius, 2013, p. 316-317.,

3. **Magomedov A.**, Urnikaitė S., Getautis V. Fulereno darinio, turinčio aktyvią 2,3-epoksipropilgrupę, sintezė. *Studentų mokslinė praktika 2012 konferencijos pranešimų santraukos, II dalis.* UAB „Lodvila", Vilnius, 2012, p. 121.,

4. **Magomedov A.**, Urnikaitė S., Getautis V. Fulereno C_{60} bei dihidrazono fragmentus turinčio puslaidininkio sintezė ir savybės. *Studentų moksliniai tyrimai 2011/2012 konferencijos pranešimų santraukos, II dalis.* UAB „Lodvila", Vilnius, 2012, p.118.,